Population Genetics Based Phylogenetics Under Stabilizing Selection for an Optimal Amino Acid Sequence: A Nested Modeling Approach

Jeremy M. Beaulieu[1,2,3], Brian C. O'Meara[2,3], Russell Zaretzki[4], Cedric Landerer[2,3], Juanjuan Chai[3,5], and Michael A. Gilchrist[2,3,*]

[1]Department of Biological Sciences, University of Arkansas, Fayetteville, AR 72701

[2]Department of Ecology & Evolutionary Biology, University of Tennessee, Knoxville, TN 37996-1610

[3]National Institute for Mathematical and Biological Synthesis, Knoxville, TN 37996-3410

[4]Department of Business Analytics & Statistics, Knoxville, TN   37996-0532

[5]Current address: 50 Main St, Suite 1039, White Plains, NY 10606

*Corresponding author: *E-mail: mikeg@utk.edu.

Associate Editor: TBD

Abstract

We present a new phylogenetic approach SelAC (Selection on Amino acids and Codons), whose substitution rates are based on a nested model linking protein expression to population genetics. Unlike simpler codon models which assume a single substitution matrix for all sites, our model more realistically represents the evolution of protein coding DNA under the assumption of consistent, stabilizing selection using cost-benefit approach. This cost-benefit approach allows us generate a set of 20 optimal amino acid specific matrix families using just a handful of parameters and naturally links the strength of stabilizing selection to protein synthesis levels, which we can estimate. Using a yeast dataset of 100 orthologs for 6 taxa, we find SelAC fits the data much better than popular models by $10^4 - 10^5$ AICc units. Our results also indicated that nested, mechanistic models better predict observed data patterns highlighting the improvement in biological realism in amino acid sequence evolution that our model provides. Additional parameters estimated by SelAC indicate that a large amount of non-phylogenetic, but biologically meaningful, information can be inferred from exisiting data. For example, SelAC prediction of gene specific protein synthesis rates correlates well with both empirical ($r = 0.33 - 0.48$) and other theoretical predictions ($r = 0.45 - 0.64$) for multiple yeast species. SelAC also provides estimates of the optimal amino acid at each site. Finally, because SelAC is a nested approach based on clearly stated biological assumptions, future modifications, such as including shifts in the optimal amino acid sequence within or across lineages, are possible.

Key words: Wright-Fisher, stabilizing selection, allele substitution, protein function, gene expression

Introduction

Phylogenetic analyses plays a critical role in most aspects of biology, particularly in the fields of ecology, evolution, paleontology, medicine, and conservation. While the scale and impact of phylogenetic studies have increased substantially over the past two decades, the realism of the mathematical models on which these analyses are based has changed relatively little by comparison. The most popular models of DNA substitution used in molecular phylogenetics are simple nucleotide models that date back to the early 1980's and 90's, e.g. F81, F84, HYK85, TN93, and GTR (see Yang (2014) for an overview), and are indifferent to the type of sequences they are fitted to. For example, when evaluating protein-coding sequences these models are inherently agnostic with regards to the different amino acid substitutions and their impact on gene function and, as a result, cannot describe the behavior of natural selection at the amino acid or protein level.

Two important and independent attempts to address this critical shortcoming were introduced by Goldman and Yang (1994, commonly abbreviated as GY) and Muse and Gaut (1994). These models were explicitly built for protein coding data, assuming that differences in the physicochemical properties between amino acids, or physicochemical distances for short, could affect substitution rates. A number of researchers have used physicochemical based models to make inferences about selection for such properties (e.g., see Blazej *et al.*, 2017; Hughes *et al.*, 1990; Koshi and Goldstein, 1997; Koshi *et al.*, 1999; McClellan and McCracken, 2001; Woolley *et al.*, 2003; Xia and Li, 1998, and Yang (2014) for a brief summary); however, in terms of tree and/or branch length reconstruction, physicochemical based codon models as originally introduced have rarely been used for empirical data. Instead, the often cited models of Goldman and Yang (1994) and Muse and Gaut (1994) have served as the basis for an array of simpler and, in turn, more popular ω models that, starting with Nielsen and Yang (1998); Yang and Nielsen (1998), typically assume an equal fixation probability for *all* non-synonymous mutations. Although often attributed to GY, these later and simpler models were the first to employ the single term ω to model the differences in fixation probability between nonsynonomous and synonomyous changes at all sites. Since their introduction, more complex models have been developed that allow ω to vary between sites or branches (as cited in Anisimova, 2012) and include selection on different synonyms for the same amino acid (e.g. Yang and Nielsen, 2008).

In Goldman and Yang (1994), Yang and Nielsen (1998), Nielsen and Yang (1998) and later studies based on their work, ω is suggested to indicate whether a given site within a protein sequence is under consistent 'stabilizing ($\omega < 1$) or 'diversifying' ($\omega > 1$) selection. Contrary to popular belief, ω does not

describe whether a site is evolving under a constant regime of stabilizing or diversifying selection, but instead how a very particular *selective environment* changes over time. Below we explain how the actual behavior of these models is inconsistent with how 'stabilizing' and 'diversifying' selection are otherwise defined and understood (e.g. see Pellmyr, 2002).

For example, when $\omega < 1$, synonymous substitutions have a higher substitution rate than any possible non-synonymous substitutions. As a result, the model behaves as if the resident amino acid i at a given site is favored by natural selection. Even when ω is allowed to vary between sites, symmetrical aspects of the model means that for any given site the strength of selection for the resident amino acid i over its 19 alternatives is equally strong regardless of their physicochemical properties. Paradoxically, natural selection for amino acid i persists *until* a substitution for another amino acid, j, occurs. As soon as amino acid j fixes, but not before, selection now favors amino acid j equally over all other amino acids, including amino acid i. This is now the opposite scenario from when i was the resident. Thus, one reasonable interpretation of ω is that it represents the rate at which the selective environment itself changes, and this change in selection at a site perfectly coincides with the fixation of a new amino acid. This change in the selective environment also differs from non-instantaneous, compensatory changes at other sites which results in reversals becoming less likely with time (Pollock *et al.*, 2012; Shah *et al.*, 2015).

Similarly, when $\omega > 1$, synonymous substitutions have a lower substitution rate than any possible non-synonymous substitutions from the resident amino acid. Again due to the model's symmetrical nature, the selection *against* the resident amino acid i is equally strong relative to alternative amino acids. The selection against the resident amino acid i persists until a substitution occurs at which point selection now *favors* amino acid i, as well as the other amino acids, to the same degree i was previously disfavored. Of course, in practice it is unlikely for the non-synonymous rate to be greater than the synonymous substitution rate in the absence of a particular process (e.g., antagonistic coevolution). Given these behaviors, ω based models are likely to only reasonably approximate a narrow set scenarios such as perfectly symmetrical over-/under-dominance or positive/negative frequency dependent selection (Hughes, 2007; Hughes and Nei, 1988; Nowak, 2006). Further, ω based models implicitly assumes the substitution is on the same timescale as the shifts in the optimal (or pessimal) amino acid. While ω is often viewed as a gene-wide metric, rather than site specific one, it is not clear to what degree this averaging mitigates these issues.

New Approaches

To address these fundamental shortcomings in ω based phylogenetic approaches, we present an approach where selection explicitly favors minimizing the cost-benefit function η of a protein whose relative performance is determined by the order and physicochemical properties of its amino acids. Our approach, which we call Selection on Amino acids and Codons or SelAC, is developed in the same vein as previous phylogenetic applications of the Wright-Fisher process (e.g. Dimmic *et al.*, 2000; Halpern and Bruno, 1998; Koshi and Goldstein, 1997; Koshi *et al.*, 1999; Lartillot and Philippe, 2004; Muse and Gaut, 1994; Rodrigue and Lartillot, 2014; Rodrigue *et al.*, 2005; Thorne *et al.*, 2012; Yang and Nielsen, 2008). Similar to Lartillot and Philippe (2004) and Rodrigue and Lartillot (2014), we assume there is a finite set of rate matrices describing the substitution process and that each position within a protein is assigned to a particular rate matrix category. Unlike that work, we assume *a priori* there are 20 different families of rate matrices, one family for when a given amino acid is favored at a site. The key parameters underlying these matrices are shared across genes with their effects scaled by each gene's expression level. By combining a cost-benefit approach with gene expresion levels, SelAC produces a large set of substitution matrices using a very limited number of parameters.

While natural selection on protein coding regions can take many forms, one general approach to describing its effects is by relating a codon sequence to the 'cost' of producing the encoded protein and the functional benefit (or potential harm) from translating its sequence. The gene specific cost of protein synthesis can be affected by the amino acids used, the direct and indirect costs of peptide assembly by the ribosome, and the use of chaperones to aid in folding. Importantly, these costs can be computed to varying degrees of realism (e.g. Lynch and Marinov, 2015; Wagner, 2005). We have previously presented models of protein synthesis costs that, alternatively, take into account the cost of ribosome pausing (Shah and Gilchrist, 2011) or premature termination errors (Gilchrist *et al.*, 2009; Gilchrist, 2007; Gilchrist and Wagner, 2006).

Protein function or 'benefit' can be affected by the amino acids at each site and their interactions. Linking amino acid sequence to protein function is a daunting task; thus for simplicity, we assume that for any given desired biological function to be carried out by a protein, that (a) the biological importance of this protein function is invariant across the tree, (b) single optimal amino acid sequence that carries out this function best, and (c) the functionality of alternative amino acid sequences declines with their physicochemical distance from the optimum on a site by site basis.

¹²³ Beyond fitting the phylogenetic data better than currently available nucleotide and codon models

¹²⁴ according to model adequacy and AICc, SelAC also makes inferences about other important biological

¹²⁵ processes. By comparing these inferences to other empirical data, such as we do with protein synthesis

¹²⁶ data, we can evaluate SelAC's performance independent of the data it is fitted to. Indeed, SelAC's

¹²⁷ assumptions lead to mechanistic and, thus, testable hypothesis about the nature of and relationships

¹²⁸ between mutation, protein function, gene expression, and rates of evolution. More importantly, alternative

¹²⁹ hypotheses could be used in place of ours and, in turn, phylogenetic and other types of data could be

¹³⁰ used to evaluate the support of these alternative models. Our hope is that by moving away from the more

¹³¹ phenomenological models we can better connect population genetics, molecular biology, and phylogenetics

¹³² allowing each area inform the others more effectively.

Results

¹³⁴ The SelAC model requires the construction of gene and amino acid specific substitution matrices that

¹³⁵ uses a submodel nested within our substitution model. This requires only a handful of genome-wide

¹³⁶ parameters such as nucleotide specific mutation rates $\mu_{i,j}$, which are scaled by effective population size

¹³⁷ N_e, amino acid side chain physicochemical weighting parameters α_c, α_p, and α_v, and a gamma distribution

¹³⁸ shape parameter α_G describing the distribution of site sensitivities G. In addition to these genome-

¹³⁹ wide parameters, the model requires a gene specific functionality expression parameter that describes

¹⁴⁰ the average rate at which the protein's functionality is produced by the organism or a gene's 'average

¹⁴¹ functionality production rate' ψ. By linking transition rates $q_{i,j}$ to gene expression ψ, our approach allows

¹⁴² use of the same model for genes under varying degrees of stabilizing selection. Specifically, we assume the

¹⁴³ strength of stabilizing selection for an optimal sequence, $\vec{a}^*$, is proportional to ψ, which we can estimate

¹⁴⁴ for each gene.

¹⁴⁵ We first evaluated the performance of our codon model by simulating datasets and estimating the

¹⁴⁶ bias of the inferred model parameters from these data. Overall, the simulation results indicated that our

¹⁴⁷ SelAC model can reasonably recover the known values of the generating model (Figures 1 and S3). This

¹⁴⁸ includes not only the parameters in SelAC, but also the optimal amino acids for a given sequence as well

¹⁴⁹ as the estimates of the branch lengths. There are, however, a few observations to note. First, the ability to

¹⁵⁰ accurately recover the true optimal amino acid sequence $\vec{a}^*$ will largely depend on the magnitude of the

¹⁵¹ realized average protein synthesis rate of the gene ϕ, which is the target functionality rate ψ divided by

¹⁵² the functionality of the observed amino acid sequence $\mathbf{B}(\vec{a})$. This is, of course, intuitive, given that ψ sets

¹⁵³ the strength of stabilizing selection towards an optimal amino acid at a site. However, the inclusion of

154 between site variation in selection via the shape parameter α_G into SelAC generally increase our estimates

155 of ψ as well as improve our ability to recover the optimal amino acids $\vec{a}^*$. This is true even for the gene

156 with the lowest baseline ψ. Second, we found a strong downward bias in estimates of α_G, which actually

157 translates to greater variation among the rate categories. The choice of a gamma distribution to represent

158 site-specific variation in sensitivity was based on mathematical convenience and convention, rather than

159 on biological reality. Further, given the fact that the density of the gamma distribution is infinite at

160 $G=0$ when $\alpha_G<1$, imputing site specific G values will be an issue in these scenarios. Nevertheless, we

161 suspect that this downward estimation bias of α_G is in large part due to the difficulty in determining

162 the baseline ψ for a given gene and the value of α_G that globally satisfies the site-specific variation in

163 sensitivity across all genes, as indicated by the slight upward bias in estimates of ψ (see Figure S5).

164 In regards to model fit in an empirical setting, our results clearly indicated that linking the

165 strength of stabilizing selection for the optimal sequence to gene expression substantially improves

166 our model fit. Further, including the shape parameter α_G for the random effects term $G\sim$

167 Gamma(shape$=\alpha_G$, rate$=\alpha_G$) to allow for heterogeneity in this selection between sites within a gene

168 improves the ΔAICc of SelAC+Γ over the simpler SelAC models by over 22,000 AIC units. Using either

169 ΔAICc or AIC$_w$ as our measure of model support, the SelAC models fit extraordinarily better than

170 GTR + Γ, GY, or FMutSel (Table 1). This is in spite of the need for estimating the optimal amino

171 acid at each position in each protein, which accounts for 49,881 additional model parameters. Even when

172 compared to the next most parameter rich codon model in our model set, FMutSel (with 178 parameters),

173 SelAC+Γ model shows over 160,000 AIC unit improvement over FMutSel. SelAC models also appeared

174 to outperform, based on likelihood and reported AIC and AICc from each program, the 161 codon models

175 in IQtree (Nguyen *et al.*, 2015). See Table S1 for results.

176 We note our use of AICc, as opposed to the standard AIC, in the above model comparisons. At

177 the outset of our study it was unclear what the appropriate sample size, n, when comparing models

178 of sequence evolution. Building upon the work of Jhwueng *et al.* (2014), our simulations suggest that

179 using the number of taxa times the number of sites as the sample size correction performed best as a

180 small sample size correction for estimating Kullback-Liebler distance in phylogenetic models (Supporting

181 Materials). This also has an intuitive appeal. In models that have at least some parameters shared across

182 sites and some parameters shared across taxa, increasing the number of sites and/or taxa should be

183 adding more samples for the parameters to estimate. This is consistent considering how likelihood is

184 calculated for phylogenetic models: the likelihood for a given site is the sum of the probabilities of each

185 observed state at each tip, which is then multiplied across sites. It is arguable that the conventional

6

approach in comparative methods is calculating AICc in the same way. That is, if only one column of data (or "site") is examined, as remains remarkably common in comparative methods, when we refer to sample size, it is technically the number of taxa multiplied by number of sites, even though it is referred to simply as the number of taxa.

With respect to estimates of gene expression SelAC, actually has two related measures. The first ψ represents the average rate at which the gene's function is produced. The second ϕ represents the average rate at which a gene's protein is produced. These two parameters are closely linked and thus highly correlated because $\phi = \psi/\mathbf{B}$ where $\mathbf{B}$ is the relative functionality of each taxa's sequence. For simplicity, we will focus on ϕ as our measure of gene expression. SelAC's ϕ values were strongly correlated with both empirical measurements (Pearson $r = 0.33 - 0.48$) and theoretical predictions (Pearson $r = 0.45 - 0.64$) of gene expression (Figure 2 and Figures S1-S2, respectively). These correlations are remarkable given that they were uncovered using only codon sequences. The estimate of the α_G parameter, which controls the shape of the site-specific, gamma-distributed, variation in sensitivity of the protein's functionality, indicated a moderate level of variation in gene expression among sites. Our estimate of $\alpha_G = 1.36$, produced a distribution of sensitivity terms G ranged from 0.342-7.32, but with more than 90% of the weight for a given site-likelihood being contributed by the 0.342 and 1.50 rate categories. In simulation, however, of all the parameters in the model, only α_G showed a consistent bias, in that the MLE were generally lower than their actual values (see Supporting Materials). Other parameters in the model, such as the Grantham weights, provide an indication as to the physicochemical distance between amino acids. Our estimates of these weights only strongly deviate from Grantham's 1974 original estimates in regards to composition weight, α_c, which is the ratio of non-carbon atoms in the end groups or rings to the number of carbon atoms in side chains. Our estimate of the composition weighting factor of $\alpha_c = 0.459$ is 1/4th the value estimate by Grantham which suggests that the substitution process is less sensitive to this physicochemical property when shared ancestry and variation in stabilizing selection are taken into account.

It is important to note that the nonsynonymous/synonymous mutation ratio, or ω, which we estimated for each gene under the FMutSel model strongly correlated with SelAC's gene expression parameter ϕ. In fact, ω showed similar, though slightly reduced correlations, with the same empirical estimates of gene expression described above (Figure 3) This would give the impression that the same conclusions could have been gleaned using a much simpler model, both in terms of the number of parameters and the assumptions made. However, as we discussed earlier, not only is this model greatly restricted in terms

of its biological feasibility, SelAC clearly performs better in terms of its fit to the data and biological realism.

For example, when we simulated the sequence for *S. cervisieae*, starting from the ancestral sequence under both GTR + Γ and FMutSel, the functionality of the simulated sequence, defined as protein function in relation to the physicochemical distance from each amino acid to the optimal, moves away from the observed sequence. By contrast, SelAC remains near the functionality of the observed sequence (Figure 4b). This is somewhat unsurprising, given that both GTR + Γ and FMutSel are agnostic to the functionality of the gene, but it does highlight the improvement in biological realism in amino acid sequence evolution that SelAC provides. We do note that the adequacy of the SelAC model does vary among individual taxa, and does not always match the observed functionality. For instance, our simulations of *S. castellii* gene function is consistently higher than estimated from the data (Figure 4c). We suspect this is an indication that assuming a single set of optimal amino acid across all taxa is too simplistic. However, we cannot rule out violations of SelAC's other model assumptions such as, a single set of Grantham weights, a single α_G, or reductions in protein functionality **B** being solely a function of physicochemical distances d between sites.

Discussion

A central goal in evolutionary biology is to quantify the nature, strength, and, ultimately, shifts in the forces of natural selection relative to genetic drift and mutation. As data set size and complexity increase, so does the amount of potential information on these forces and their dynamics. As a result, there is a need for more complex and realistic models to accomplish this goal (Goldman *et al.*, 1996, 1998; Halpern and Bruno, 1998; Lartillot and Philippe, 2004; Thorne *et al.*, 1996). Although extremely popular due to their elegance and computational efficiency, the utility of ω based models in helping us reach this goal is substantially more limited than commonly recognized. Because these ω models use a single substitution matrix, they are only applicable for situations in which the substitution process and shifts in the selective environment are intrinsic to the sequence, such as with positive or negative frequency dependent selection; these models do not describe stabilizing or diversifying selection as commonly envisioned (Endler, 1986; Pellmyr, 2002).

Starting with Halpern and Bruno (1998), a number of researchers have developed methods for linking heterogenous or site-specific selection on protein sequence and phylogenetics (e.g. Dimmic *et al.*, 2000; Koshi and Goldstein, 2000; Koshi *et al.*, 1999; Lartillot and Philippe, 2004; Robinson *et al.*, 2003; Rodrigue and Lartillot, 2014; Thorne *et al.*, 2012; Yang *et al.*, 1998). Halpern and Bruno (1998) calculated a vector

of 20 expected amino acid frequencies for each amino acid site, making it the most general and most parameter rich of these methods. This generality, however, comes at the cost of being purely descriptive; there is no explicit biological mechanism proposed to explain the site specific amino acid frequencies estimated. By grouping together amino sites with similar evolutionary behaviors, Lartillot and Philippe (2004) and Rodrigue and Lartillot (2014) retained the descriptive nature of Halpern and Bruno (1998) work while greatly reduced the number of model parameters needed.

SelAC follows in this tradition of using multiple substitution matrices, but includes some key advances. First, by nesting a model of a sequence's cost-benefit function $\mathbf{C}/\mathbf{B}$ within a broader model, SelAC allows us to formulate and test a hierarchical, mechanistic models of stabilizing selection. More precisely, our nested approach allows us to relax the assumption that physicochemical deviations from the optimal sequence $\vec{a}^*$ are equally disruptive at all sites within a protein. Indeed, SelAC results are consistent with the idea that the strength of stabilizing selection against physicochemical deviations from $\vec{a}^*$ varies between sites (ΔAICc = 20,983; Table 1). Second, because our substitution matrices are built on a formal description of a sequence's cost-benefit function $\mathbf{C}/\mathbf{B}$, we are able to efficiently parameterize 20 different matrices using a relatively small number of genome-wide parameters – e.g. our physicochemical weightings, α_c, α_p, and α_v, and the shape parameter α_G for the distribution of selective strength G and one gene specific expression parameter ψ. While the $\mathbf{C}/\mathbf{B}$ function on which SelAC currently rests is very simple, nevertheless, it leads to a dramatic increase in our ability to explain the sequence data we analyzed. Importantly, because SelAC uses a formal description of a sequence's $\mathbf{C}/\mathbf{B}$, replacing our assumptions with more sophisticated ones in the future is relatively straightforward. Third, our use of nested models also allows us to make biologically meaningful and testable predictions. By linking a gene's expression level to the strength of purifying selection it experiences, we are able to provide coarse estimates of gene expression. The anticorrelation between ω and gene expression indicates ω is often just a proxy for the strength, rather than nature, natural selection on a sequence.

Thus, we believe our cost-benefit approach to be a substantial advance of the more simplistic ω models, is complementary to the work of others in the field (e.g. Rodrigue and Lartillot, 2014; Thorne *et al.*, 2012), and, in turn, lays the foundation for more realistic work in the future. For instance, by assuming there is an optimal amino acid for each site, SelAC naturally leads to a non-symmetrical and, thus, more cogent model of protein sequence evolution. Because the strength of selection depends on an additive function of amino acid physicochemical properties, an amino acid more similar to the optimum has a higher probability of replacing a more dissimilar amino acid than the converse situation. Further, SelAC

does not assume the system is always at the optimum or pessimum point of the fitness landscape, as occurs when $\omega < 1$ or > 1, respectively.

Importantly, the cost-benefit approach underlying SelAC allows us to link the strength of selection on a protein sequence to its gene's expression level. Despite its well recognized importance in determining the rate of protein evolution (e.g. Drummond *et al.*, 2005, 2006), phylogenetic models have ignored the fact that expression levels vary between genes. In order to link gene expression and the strength of stabilizing selection on protein sequences, we simply assume that the strength of selection on a gene is proportional to the average protein synthesis rate of the gene.

One possible mechanism with some theoretical and empirical support which generates a linear relationship between the strength of selection and gene expression is the assumption of compensatory gene expression (Allison, 2012; Allison and Goulden, 2017; Brown and Elliot, 1997; King *et al.*, 2015; Lerman *et al.*, 2012; Thiele *et al.*, 2012; Zanger and Schwab, 2013). That is, the assumption that any reduction in protein function is compensated for by an increase in the protein's production rate and, in turn, abundance. For example, a mutation which reduces the functionality of the protein to 90% of the optimal protein, would require $1/0.9 = 1.11$ of these suboptimal proteins to be produced relative to the optimal protein in order to maintain the same amount of that protein's functionality in the cell. Because the energetic cost of an 11% increase in a protein's synthesis rate is proportional to its target synthesis rate, our assumptions naturally link changes in protein functionality and changes in gene expression and its associated costs. Such a response has been shown when error rates during protein production increases, however, the generality of such a response has to be determined (Goldsmith and Tawfik, 2009). Further, our model does not consider additional costs such as those imposed by misfoled proteins (Drummond and Wilke, 2008). Nevertheless, the fact that our method allows us to explain 13-23% of the variation in gene expression measured using RNA-Seq, suggests that our assumption of cell compensation via increased expression is a reasonable starting point.

Furthermore, by linking expression and selection, SelAC provides a natural framework for combining information from protein coding genes with very different rates of evolution; from low expression genes providing information on shallow branches to high expression genes providing information on deep branches. This is in contrast to a more traditional approach of concatenating gene sequences together, which is equivalent to assuming the same average functionality production rate ψ for all of the genes, or more recent approaches where different models are fitted independently to different genes. Our results indicate that including a gene specific ψ value vastly improves SelAC fits (Table 1). Perhaps more convincingly, we find that the target functionaly production rate ψ and the realized average protein

synthesis rate $\phi = \psi/\mathbf{B}$ are reasonably well correlated with laboratory measurements and theoretical predictions of gene expression (Pearson $r = 0.34 - 0.64$; Figures 2, S1, and S2). The idea that quantitative information on gene expression is embedded within intra-genomic patterns of synonymous codon usage is well accepted; our work shows that this information can also be extracted from comparative data at the amino acid level.

Of course, given the general nature of SelAC and the complexity of biological systems, other biological forces besides selection for reducing energy flux likely contribute to intergenic variation in the magnitude of stabilizing selection. Similarly, other physicochemical properties besides composition, volume, and charge likely contribute to site specific patterns of amino acid substitution. For example, Blazej *et al.* (2017) have developed substitution matrices using various physicochemical properties. Thus, a larger and more informative set of physicochemical weights might improve our model fit and reduce the noise in our estimates of realized protein synthesis rates ϕ. Even if other physicochemical properties are considered, the idea of a consistent, genome wide physicochemical weighting of these terms seems highly unlikely. Since the importance of an amino acid's physicochemical properties likely changes with its position in a folded protein, one way to incorporate such effects is to test whether the data supports multiple sets of physicochemical weights for either subsets of genes or regions within genes, rather than a single set.

Both of these points highlight the advantage of the detailed, mechanistic modeling approach underlying SelAC. Because there is a clear link between protein expression, synthesis cost, and functionality, SelAC can be extended by increasing the realism of the mapping between these terms and the coding sequences being analyzed. For example, SelAC currently assumes the optimal amino acid for any site is fixed along all branches. This assumption can be relaxed by allowing the optimal amino acid to change during the course of evolution along a branch. From a computational standpoint, the additive nature of selection between sites is desirable because it allows us to analyze sites within a gene largely independently of each other. From a biological standpoint, this additivity between sites ignores any non-linear interactions between sites, such as epistasis, or between alleles, such as dominance. Thus, our work can be considered a first step to modeling these more complex scenarios.

For example, our current implementation ignores any selection on synonymous codon usage bias (CUB) (c.f. Pouyet *et al.*, 2016; Yang and Nielsen, 2008). Including such selection is tricky because introducing the site-specific cost effects of CUB, which is consistent with the hypothesis that codon usage affects the efficiency of protein assembly or $\mathbf{C}$, into a model where amino acids affect protein function or $\mathbf{B}$, results in a cost-benefit ratio $\mathbf{C}/\mathbf{B}$ with epistatic interactions between all sites. These epistatic effects can likely be ignored under certain conditions or reasonably approximated based on an expectation of

11

codon specific costs (e.g. Kubatko *et al.*, 2016). Nevertheless, it is difficult to see how one could identify such conditions without modeling the way in which codon and amino acid usage affects $\mathbf{C}/\mathbf{B}$.

This work also points out the potential importance of further investigation into model choice in phylogenetics. For likelihood models, use of AICc has become standard. However, how one determines the appropriate number of data points in a model is more complicated than generally recognized. Common sense suggests that dataset size is increased by adding taxa and/or sites. In other words, a dataset of 1000 taxa and 100 sites must have more information on substitution models than a dataset of 4 taxa and 100 sites. Our simple analyses support the hypothesis that the number of observations in a dataset (number of sites $\times$ number of taxa) should be taken as the sample size for AICc, but this conclusion likely only applies when there is sufficient independence between taxa. For instance, one could imagine a phylogeny where one taxon is sister to a polytomy of 99 taxa that have zero length terminal branches. Absent measurement error or other intraspecific variation, one would have 100 species but only two unique trait values, and the only information about the process of evolution comes from what happens on the path connecting the lone taxon to the polytomy. Although this is a rather extreme example, it seems prudent for researchers to use a simulation based approach similar to the one we take here to determine the appropriate means for calculating the effective number of data points in their data.

There are still significant shortcomings in the approach outlined here. Most worrisome are biological oversimplifications in SelAC. For example, at its heart, SelAC assumes that suboptimal proteins can be compensated for, at a cost, simply by producing more of them. However, this is likely only true for proteins reasonably close to the optimal sequence. Different enough proteins will fail to function entirely: the active site will not sufficiently match its substrates, a protein will not properly pass through a membrane, and so forth. Yet, in our model, even random sequences still permit survival via an increased rate of protein production. Another deficiency is the assumption of site independence and unchanging optimal amino acids through time, neither of which matches reality (Pollock *et al.*, 2012; Shah *et al.*, 2015). We assume single nucleotide changes only, despite evidence from Kosiol *et al.* (2007) and Whelan and Goldman (2004) that better fit can be accomplished by allowing instantaneous mutations of multiple nucleotides simultaneously. Like the other oversimplifications previously discussed, these assumptions can be relaxed through further extension of this model.

A deeper potential issue comes from the nature of model fitting itself. Because SelAC, like all models, is built on very particular assumptions, it is likely these assumptions are violated in many, if not most, cases. While all models are incomplete descriptions of reality and, thus, wrong (Box, 1976), our aim with SelAC is to provide a model that is 'less wrong' (Asimov, 1989). Because SelAC's assumptions result

in a model that is more consistent with the data, our analyses supports this idea. While 'less wrong', caution should be taken when interpreting SelAC's model parameters since the model itself is admittedly incomplete. In addition, other biological mechanisms could result in similar, if not identical, mathematical representations (Beaulieu and O'Meara, 2016; Rabosky and Goldberg, 2015) which, in turn, illustrates one limit to comparative sequence analysis.

There are also deficiencies in our implementation. Though reasonable to use for a given topology with 10's of species, it is currently too slow for practical use for large tree searches. Our work serves as a proof of concept, or of utility for targeted questions where a more realistic model may be of use (placement of particular taxa, for example). Future work will encode SelAC models into a variety of mature, popular tree-search programs. SelAC also represents a challenging optimization problem: the nested models reduce parameter complexity vastly, but there are still numerous parameters to optimize, including the discrete parameter of the optimal amino acid at each site. One way to avoid the use of discrete parameters at the expense of more of them would be to have SelAC estimate the optimum physicochemical values on a per site basis rather than a specific amino acid. While this would increase the number of parameters estimated, it would have the practical advantage of continuous parameter optimization rather than discrete. More importantly, biologically such a model would be more realistic (as it is the properties that selection "sees", not the identity of the amino acid itself).

In spite of these difficulties, SelAC represents an important step in uniting phylogenetic and population genetic models (Higgs, 2008). Most work in this area use a given tree to make inferences about the nature or distribution of selection coefficients (Blazej *et al.*, 2017; Hughes *et al.*, 1990; McClellan and McCracken, 2001; Woolley *et al.*, 2003; Xia and Li, 1998, e.g.). While the work of Koshi *et al.* (1999), Dimmic *et al.* (2000), Koshi and Goldstein (2000), Robinson *et al.* (2003), Lartillot and Philippe (2004), Thorne *et al.* (2012), and Rodrigue and Lartillot (2014) do involve tree inferences, are all models of constant, stabilizing selection, SelAC can be generalized further to include diversifying selection. Specifically, by letting SelAC's sensitivity term G, which we now assume is ≥ 0, to take on negative values, SelAC will behave as if there is a pessimal, rather than optimal, amino acid for the given site. In this diversifying selection scenario, amino acids with physicochemical qualities more dissimilar to the pessimal amino acid are increasingly favored, potentially resulting in multiple fitness peaks.

The ability to extend our model and, in turn, sharpen our thinking about the nature of natural selection on amino acid sequences illustrates the value of moving from descriptive to more mechanistic models in general and phylogenetics in particular. How frequently diversifying selection of this nature occurs is an open, but addressable, question. Regardless of the frequency at which diversifying selection occurs,

⁴⁰⁷ another question of interest to evolutionary biologists is, "How often does the optimal/pessimal amino

⁴⁰⁸ sequence change along any given branch?" Due to its mechanistic nature, SelAC can also be extended

⁴⁰⁹ to include changes in the optimal/pessimal sequence over a phylogeny using a hidden Markov modelling

⁴¹⁰ approach (Penny *et al.*, 2001; Tuffley and Steel, 1998; Whelan, 2008, for an explicit shift the optimal

⁴¹¹ sequence see Tamuri *et al.* (2009)). Extending SelAC in these ways, will allow researchers to explicitly

⁴¹² model shifts in selection on protein sequences and, in turn, quantify their frequency and magnitude

⁴¹³ thus deepening our understanding of biological evolution. Such approaches would be challenging using

⁴¹⁴ non-mechanistic and parameter rich models which infer up to 19 different parameters per site category

⁴¹⁵ (Halpern and Bruno, 1998; Rodrigue and Lartillot, 2014; Tamuri *et al.*, 2012, 2014).

⁴¹⁶ In summary, SelAC allows biologically relevant population genetic parameters to be estimated from

⁴¹⁷ phylogenetic information, while also dramatically improving fit and accuracy of phylogenetic models. By

⁴¹⁸ explicitly modeling the optimal/pessimal sequence of a gene, SelAC can be extended to include shifts

⁴¹⁹ in the optimal/pessimal sequence over evolutionary time. Moreover, it demonstrates that there remains

⁴²⁰ substantially more information in the coding sequences used for phylogenetic analysis than other methods

⁴²¹ can access. Given the enormous amount of efforts expended to generate sequence datasets, it makes sense

⁴²² for researchers to continue developing more realistic models of sequence evolution in order to extract the

⁴²³ biological information embedded in these datasets. The cost-benefit model we develop here is just one of

⁴²⁴ many possible paths of mechanistic model development.

Materials & Methods

Overview

⁴²⁷ We model the substitution process as a classic Wright-Fisher process which includes the forces

⁴²⁸ of mutation, selection, and drift (Berg and Lässig, 2003; Fisher, 1930; Iwasa, 1988; Kimura, 1962;

⁴²⁹ McCandlish and Stoltzfus, 2014; Sella and Hirsh, 2005; Wright, 1969). For simplicity, we ignore linkage

⁴³⁰ effects and, as a result of this and other assumptions, sequences evolve in a site independent manner.

⁴³¹ Because SelAC requires twenty families of 61×61 matrices, the number of parameters needed to

⁴³² implement SelAC would, without further assumptions, be extremely large (i.e. on the order of 74,000

⁴³³ parameters). To reduce the number of parameters needed, while still maintaining a high degree of

⁴³⁴ biological realism, we construct our gene and amino acid specific substitution matrices using a submodel

⁴³⁵ nested within our substitution model, similar to approaches in Gilchrist (2007); Gilchrist *et al.* (2015);

⁴³⁶ Shah and Gilchrist (2011).

⁴³⁷ One advantage of a nested modeling framework is that it requires only a handful of genome-wide

⁴³⁸ parameters such as nucleotide specific mutation rates (scaled by effective population size N_e), amino acid

14

side chain physicochemical weighting parameters, and a shape parameter describing the distribution of site sensitivities. In addition to these genome-wide parameters, SelAC requires a gene specific functionality expression parameter ψ which describes the average rate at which the protein's functionality is produced by the organism or a gene's 'average functionality production rate' for short. Currently, ψ is fixed across the phylogeny, though relaxing this assumption is a goal of future work. The gene specific parameter ψ is multiplied by additional model terms to make a composite term ψ' which scales the strength and efficacy of selection for the optimal amino acid sequence relative to drift (see Implementation below). In terms of the functionality of the protein encoded, we assume that for any given gene there exists an optimal amino acid sequence $\vec{a}^*$ and that, by definition, a complete, error free peptide consisting of $\vec{a}^*$ provides one unit of the gene's functionality. We also assume that natural selection favors genotypes that are able to synthesize their proteome more efficiently than their competitors and that each savings of an high energy phosphate bond per unit time leads to a constant proportional gain in fitness A_0 (which was q in our previous work Gilchrist (2007)). SelAC also requires the specification (as part of parameter optimization) of an optimal amino acid a^* at each position within a coding sequence. This requirement of one a^* per site makes our $\vec{a}^*$ the largest category of parameters SelAC estimates. Despite the need to specify a^* for each site, because we use a submodel to derive our substitution matrices, SelAC estimates a relatively small number of the parameters when compared to more general approaches where the fitness of each amino acid is allowed to vary freely of any physicochemical properties (Halpern and Bruno, 1998; Lartillot and Philippe, 2004; Rodrigue and Lartillot, 2014).

As with other phylogenetic methods, SelAC generates estimates of branch lengths and nucleotide specific mutation rates. In addition, the method can also be used to make quantitative inferences on the optimal amino acid sequence of a given protein as well as the realized average synthesis rate of each protein used in the analysis. The mechanistic basis of SelAC also means it can be easily extended to include more biological realism and test more explicit hypotheses about sequence evolution.

Mutation Rate Matrix μ

We begin with a 4x4 nucleotide mutation matrix that describes mutation rates between different bases and, in turn, different codons. For our purposes, we rely on the general unrestricted model (UNREST from Yang, 1994) because it imposes no constraints on the instantaneous rate of change between any pair of nucleotides. More constrained models, such as the Jukes-Cantor (JC), Hasegawa-Kishino-Yano (HKY), or the general time-reversible model (GTR), could also be used.

The 12 parameter UNREST model defines the relative rates of change between a pair of nucleotides. Thus, we arbitrarily set the G→T mutation rate to 1, resulting in 11 free mutation rate parameters in the

4x4 mutation nucleotide mutation matrix. The nucleotide mutation matrix is also scaled by a diagonal matrix $\boldsymbol{\pi}$ whose entries, $\pi_{i,i}$, correspond to the equilibrium frequencies of each base. These equilibrium nucleotide frequencies are determined by analytically solving $\boldsymbol{\pi} \times \mathbf{Q} = 0$. We use this $\mathbf{Q}$ to populate a 61×61 codon mutation matrix $\boldsymbol{\mu}$, whose entries $\mu_{i,j}$ $i \neq j$ describes the mutation rate from codon i to j and $\mu_{i,i} = -\sum_j \mu_{i,j}$. We generate this matrix using a "weak mutation" assumption, such that evolution is mutation limited, codon substitutions only occur one nucleotide at a time. As a result, the rate of change between any pair of codons that differ by more than one nucleotide is zero.

While the overall model does not assume equilibrium, we still need to scale our mutation matrices $\boldsymbol{\mu}$ by a scaling factor S. As traditionally done, we rescale our time units such that at equilibrium, one unit of branch length represents one expected mutation per site (which equals the substitution rate under neutrality). More explicitly, $S = -\left(\sum_{i \in \text{codons}} \mu_{i,i} \pi_{i,i}\right)$ where the final mutation rate matrix is the original mutation rate matrix multiplied by $1/S$.

Protein Synthesis Cost-Benefit Function η

SelAC links fitness to the product of the cost-benefit function of a gene η and the organism's average target synthesis rate of the functionality provided by gene ψ. As a result, the average flux energy an organism spends to meet its target functionality provided by the gene is $\eta \times \psi$. Compensatory changes that allow an organism to maintain functionality even with loss of one or both copies of a gene are widespread. There is evidence of compensation for protein function. Metabolism with gene expression models (ME-models) link those factors to successfully make predictions about response to perturbations in a cell (King *et al.*, 2015; Lerman *et al.*, 2012). For example, an ME-model for *E. coli* successfully predicted gene expression levels in vivo (Thiele *et al.*, 2012). Here we assume that for finer scale problems than entire loss (for example, a 10% loss of functionality) the compensation is more production of the protein. The particular type of dosage compansation assumed by SelAC in responds to stress (e.g. reduced functionality) is commonly assumed in microbial ecology (Allison, 2012; Allison and Goulden, 2017). Our assumption is also consistent with the Michaelis-Menten enzyme kinetics. Moreover, there is evidence that mutations can influence expression level, though this does not always match our expression compensation assumption (Brown and Elliot, 1997; Zanger and Schwab, 2013). In order to link genotype to our cost-benefit function $\eta = \mathbf{C}/\mathbf{B}$, we begin by defining our benefit function $\mathbf{B}$.

Benefit: Our benefit function $\mathbf{B}$ measures the functionality of the amino acid sequence $\vec{a}_i$ encoded by a set of codons $\vec{c}_i$, i.e. $a(\vec{c}_i) = \vec{a}_i$ relative to that of an optimal sequence $\vec{a}^*$. By definition, $\mathbf{B}(\vec{a}^*|\vec{a}^*) = 1$ and $\mathbf{B}(\vec{a}_i|\vec{a}^*) < 1$ for all other sequences. We assume all amino acids within the sequence contribute to protein

16

function and that this contribution declines as an inverse function of physicochemical distance from each amino acid to the optimal one. Formally, we assume that

$$\mathbf{B}(\vec{a}|\vec{a}^*) = \left(\frac{1}{n} \sum_{p=1}^{n} \left(1 + G_p d(a_p, a_p^*) \right) \right)^{-1} \tag{1}$$

where n is the length of the protein, $d(a_p, a_p^*)$ is a weighted physicochemical distance between the amino acid encoded at a given position p and a_p^* is the optimal amino acid for that position. There are many possible measures for physiochemical distance; we use Grantham (1974) distances by default, though others may be chosen. For simplicity, we assume all nonsense mutations are lethal by defining the the physicochemical distance between a stop codon and a sense codon as ∞. The term G_p describes the sensitivity of the protein's function to physicochemical deviation from the optimimum at site position p. We assume that $G_p \sim \mathrm{Gamma}(\mathrm{shape} = \alpha_G, \mathrm{rate} = \alpha_G)$ in order to ensure $\mathbb{E}(G_p) = 1$. Given the definition of the Gamma distribution, the variance in G_p is equal to shape/rate$^2 = 1/\alpha_G$. We note that at the limit of $\alpha_G \to \infty$, the model becomes equivalent to assuming uniform site sensitivity where $G_p = 1$ for all positions p. Further, $\mathbf{B}(\vec{a}_i|\vec{a}^*)$ is inversely proportional to the average physicochemical deviation of an amino acid sequence $\vec{a}_i$ from the optimal sequence $\vec{a}^*$ weighted by each site's sensitivity to this deviation. $\mathbf{B}(\vec{a}_i|\vec{a}^*)$ can be generalized to include second and higher order terms of the distance measure d.

Cost: Protein synthesis involves both direct and indirect assembly costs. Direct costs consist of the high energy phosphate bonds $\sim P$ of ATPs or GTPs used to assemble the ribosome on the mRNA, charge tRNA's for elongation, move the ribosome forward along the transcript, and terminate protein synthesis. As a result, direct protein assembly costs are the same for all proteins of the same length. Indirect costs of protein assembly are potentially numerous and could include the cost of amino acid synthesis as well the cost and efficiency with which the protein assembly infrastructure such as ribosomes, aminoacyl-tRNA synthetases, tRNAs, and mRNAs are used. When these indirect costs are combined with sequence specific benefits, the probability of a mutant allele fixing is no longer independent of the rest of the sequence (Gilchrist *et al.*, 2015) and, as a result, model fitting becomes substantially more complex. Thus for simplicity, in this study we ignore indirect costs of protein assembly that vary between genotypes and define,

$$\mathbf{C}(\vec{c}_i) = \text{Direct energetic cost of protein synthesis.}$$

$$= A_1 + A_2 n$$

527 where, A_1 and A_2 represent the direct cost, in high energy phosphate bonds, of ribosome initiation and

528 peptide elongation, respectively, where $A_1 = A_2 = 4 \sim P$.

Defining Physicochemical Distances

530 Assuming that functionality declines with an amino acid a_i's physicochemical distance from the

531 optimum amino acid a^* at each site provides a biologically defensible way of mapping genotype to protein

532 function that requires relatively few free parameters. In addition, SelAC naturally lends itself to model

533 selection since one could compare the quality of SelAC fits using different mixtures of physicochemical

534 properties. Following (Grantham, 1974), we focus on using composition c, polarity p, and molecular

535 volume v of each amino acid's side chain residue to define our distance function, but the model and

536 its implementation can flexibly handle a variety of properties. We use the Euclidian distance between

537 residue properties where each property c, p, and v has its own weighting term, α_c, α_p, α_v, respectively,

538 which we refer to as 'Grantham weights'. Because physicochemical distance is ultimately weighted by a

539 gene's specific average protein synthesis rate ψ, another parameter we estimate, there is a problem with

540 parameter identifiablity. The scale of gene expression is affected by how we measure physicochemical

541 distances which, in turn, is determined by our choice of Grantham weights. As a result, by default we

542 set $\alpha_v = 3.990 \times 10^{-4}$, the value originally estimated by Grantham, and recognize that our estimates of

543 α_c and α_p and ψ are scaled relative to this choice for α_v. More specifically,

$$d(a_i, a^*) = \sqrt{\alpha_c [c(a_i) - c(a^*)]^2 + \alpha_p [p(a_i) - p(a^*)]^2 + \alpha_v [v(a_i) - v(a^*)]^2}.$$

Linking Protein Synthesis to Allele Substitution

545 Next we link the protein synthesis cost-benefit function η of an allele with its fixation probability.

546 First, we assume that each protein encoded within a genome provides some beneficial function and that

547 the organism needs that functionality to be produced at a target average rate ψ. Again, by definition,

548 the optimal amino acid sequence for a given gene, $\vec{a}^*$, produces one unit of functionality, i.e. $\mathbf{B}(\vec{a}^*) = 1$.

549 Second, we assume that the actual average rate a protein is synthesized ϕ is regulated by the organism

550 to ensure that functionality is produced at rate ψ. As a result, it follows that $\phi = \psi / \mathbf{B}(\vec{a}|\vec{a}^*)$ and the

551 energetic burden of a suboptimal amino acid increases the more it decreases the protein's functionality,

552 $\mathbf{B}$. In other words, the average production rate of a protein $\vec{a}$ with relative functionality $\mathbf{B}(\vec{a}) < 1$ must

553 be $1/\mathbf{B}(\vec{a}|\vec{a}^*)$ times higher than the production rate needed if the optimal amino acid sequence $\vec{a}^*$ was

554 encoded since $\mathbf{B}(\vec{a}^*|\vec{a}^*) = 1$. For example, a cell with an allele $\vec{a}$ where $\mathbf{B}(\vec{a}|\vec{a}^*) = 9/10$ would have to

555 produce the protein at rate $\phi = 10/9 \times \psi = 1.11\psi$. Similarly, a cell with an allele $\vec{a}$ where $\mathbf{B}(\vec{a}|\vec{a}^*) = 1/2$

18

556 will have to produce the protein at $\phi = 2\psi$. In contrast, a cell with the optimal allele $\vec{a}^*$ would have to

557 produce the protein at rate $\phi = \psi$.

558   Third, we assume that every additional high energy phosphate bond, $\sim P$, spent per unit time to meet

559 the organism's target function synthesis rate ψ leads to a slight and proportional decrease in fitness W.

560 This assumption, in turn, implies

$$W_i(\vec{c}) \propto \exp[-A_0 \eta(\vec{c}_i)\psi].$$

561 where A_0 describes the proportional decline in fitness with every $\sim P$ wasted per unit time. Because A_0

562 shares the same time units as ψ and ϕ and only occurs in SelAC in conjunction with ψ, we do not need

563 to explicitly identify our time units. Instead, we recognize that our estimates of ψ share an unknown

564 scaling term.

565   Correspondingly, the ratio of fitness between two genotypes is,

$$W_i/W_j = \exp[-A_0 \eta(\vec{c}_i)\psi] / \exp[-A_0 \eta(\vec{c}_j)\psi]$$

$$= \exp[-A_0(\eta(\vec{c}_i) - \eta(\vec{c}_j))\psi]$$

566 Given our formulations of $\mathbf{C}$ and $\mathbf{B}$, the fitness effects between sites are multiplicative and, therefore, the

567 substitution of an amino acid at one site can be modeled independently of the amino acids at the other

568 sites within the coding sequence. As a result, the fitness ratio for two genotypes differing at multiple sites

569 simplifies to

$$W_i/W_j = \exp\left[-\left(\frac{A_0(A_1 + A_2 n)}{n}\right) \sum_{p \in \mathbb{P}} [d(a_{i,p}, a_p^*) - d(a_{j,p}, a_p^*)] G_p \psi\right]$$

570 where $\mathbb{P}$ represents the codon positions in which $\vec{c}_i$ and $\vec{c}_j$ differ. Fourth, we make a weak mutation

571 assumption, such that alleles can differ at only one position at any given time, i.e. $|\mathbb{P}| = 1$, and that the

572 population is evolving according to a Wright-Fisher process. As a result, the probability a new mutant,

573 j, introduced via mutation into a resident population i with effective size N_e will go to fixation is,

$$u_{i,j} = \frac{1 - (W_i/W_j)^b}{1 - (W_i/W_j)^{2N_e}}$$

$$= \frac{1 - \exp\left\{-\frac{A_0}{n}(A_1 + A_2 n)[d(a_i, a^*) - d(a_j, a^*)]G_p \psi b\right\}}{1 - \exp\left\{-\frac{A_0}{n}(A_1 + A_2 n)[d(a_i, a^*) - d(a_j, a^*)]G_p \psi 2N_e\right\}}$$

574 where $b = 1$ for a diploid population and 2 for a haploid population (Berg and Lässig, 2003; Iwasa, 1988;

575 Kimura, 1962; Sella and Hirsh, 2005; Wright, 1969). Finally, assuming a constant mutation rate between

576 alleles i and j, $\mu_{i,j}$, the substitution rate from allele i to j can be modeled as,

$$q_{i,j} = \frac{2}{b}\mu_{i,j}N_e u_{i,j}.$$

where, given the substitution model's weak mutation assumption, $N_e\mu \ll 1$. In the end, each optimal amino acid has a separate 61×61 substitution rate matrix $\mathbf{Q}_a$, which incorporates selection for the amino acid (and the fixation rate matrix this creates) as well as the common mutation parameters across optimal amino acids. This results in the creation of 20 $\mathbf{Q}$ matrices, one for each amino acid and each with 3,721 entries which are based on a relatively small number of model parameters (one to 11 mutation rates, two free Grantham weights, the cost of protein assembly, A_1 and A_2, the gene specific target functionality synthesis rate ψ, and optimal amino acid at each position p, a_p^*). These model parameters can either be specified *a priori* and/or estimated from the data.

Given our assumption of independent evolution among sites, it follows that the probability of the whole data set is the product of the probabilities of observing the data at each individual site. Thus, the likelihood $\mathcal{L}$ of amino acid a being optimal at a given site position p is calculated as

$$\mathcal{L}(\mathbf{Q}_a|\mathbf{D}_p,\mathbf{T}) \propto \mathbf{P}(\mathbf{D}_p|\mathbf{Q}_a,\mathbf{T}) \tag{2}$$

In this case, the data, $\mathbf{D}_p$, are the observed codon states at position p for the tips of the phylogenetic tree with topology $\mathbf{T}$. For our purposes we take $\mathbf{T}$ as given, but it could be estimated as well. The pruning algorithm of Felsenstein (1981) is used to calculate $\mathcal{L}(\mathbf{Q}_a|\mathbf{D}_p,\mathbf{T})$. The log of the likelihood is maximized by estimating the genome scale parameters which consist of 11 mutation parameters, which are implicitly scaled by $2N_e/b$, and two Grantham distance parameters, α_c and α_p, and the sensitivity distribution parameter α_G. Because A_0 and ψ always co-occur and are scaled by N_e, for each gene we estimate a composite term $\psi' = A_0\psi N_e b$ and the optimal amino acid for each position a_p^* of the protein. When estimating α_G, the likelihood then becomes the average likelihood which we calculate using the generalized Laguerre quadrature with $k=4$ points (Felsenstein, 2001).

Finally, we note that because we infer the ancestral state of the system, our approach does not rely on any assumptions of model stationarity. Nevertheless, as our branch lengths grow the probability of observing a particular amino acid a at a given site approaches a stationary value proportional to $W(a)^{2N_e-b}$ and any effects of mutation bias (Sella and Hirsh, 2005).

Implementation

All methods described above are implemented in the new R package, `selac` available through GitHub (`https://github.com/bomeara/selac`) which will be uploaded to CRAN once peer review has completed. Our package requires as input a set of fasta files that each contain an alignment of coding sequence for a set of taxa, and the phylogeny depicting the hypothesized relationships among them. In addition to the SelAC models, we implemented the GY codon model of Goldman and Yang (1994), the

20

FMutSel mutation-selection model of Yang and Nielsen (2008), and the standard general time-reversible nucleotide model that allows for Γ distributed rates across sites. These likelihood-based models represent a sample of the types of popular models often fit to codon data.

For the SelAC models, the starting guess for the optimal amino acid at a site comes from 'majority' rule, where the initial optimum is the most frequently observed amino acid at a given site (ties resolved randomly). Our optimization routine utilizes a four stage hill climbing approach. More specifically, within each stage a block of parameters are optimized while the remaining parameters are held constant. The first stage optimizes the block of branch length parameters. The second stage optimizes the block of gene specific composite parameters $\psi' = A_0 \psi N_e b$. The third stage optimizes SelAC's parameters shared across the genome α_c and α_p, and the sensitivity distribution parameter α_G. The fourth stage estimates the optimal amino acid at each site a^*. This entire four stage cycle is repeated up to six more times, using the estimates from the previous cycle as the initial conditions for the new one. The search is terminated when the improvement in the log-likelihood between cycles is less than 10^{-8} at which point we consider the ML solution found and the search is terminated. For optimization of a given set of parameters, we rely on a bounded subplex routine (Rowan, 1990) in the package `NLoptR` (Johnson, 2012) to maximize the log-likelihood function. To ensure the robustness of our results, we perform a set of independent analyses with different sets of naive starting points with respect to the gene specific composite ψ' parameters, α_c, and α_p and were able to repeatedly reach the same log-likelihood (lnL) peak in our parameter space. Confidence in the parameter estimates can be generated by an 'adaptive search' procedure that we implemented to provide an estimate of the parameter space that is some pre-defined likelihood distance (e.g., 2 lnL units) from the maximum likelihood estimate (MLE), which follows Beaulieu and O'Meara (2016) and Edwards (1984).

We note that our current implementation of SelAC is slow, and is best suited for data sets with relatively small number of taxa (i.e. 10's not 100's). This limitation is largely due to the size and quantity of matrices we create and manipulate to calculate the log-likelihood of an individual site. Ongoing work will address the need for speed, with the eventual goal of implementing SelAC in popular phylogenetic inference toolkits, such as RevBayes (Hoehna *et al.*, 2016), PAML (Yang, 2007) and RAxML (Stamatakis, 2006).

Simulations

We evaluated the performance of our codon model by simulating datasets and estimating the bias of the inferred model parameters from these data. Our 'known' parameters under a given generating model were based on fitting SelAC to the 106 gene data set and phylogeny of Rokas *et al.* (2003). The tree used in these analyses is outdated with respect to the current hypothesis of relationships within

Saccharomyces, but we rely on it simply as a training set that is separate from our empirical analyses (see section below). Bias in the model parameters were assessed under two generating models: one where we assumed a model of SelAC with uniform sensitivity across sites (i.e. $G_p = 1$ for all sites, i.e. $\alpha_G = \infty$), and one where we used the Gamma distribution joint shape and rate parameter α_G estimated from the empirical data. Under each of these two scenarios, we used parameter estimates from the corresponding empirical analysis and simulated 50 five-gene data sets. For the gene specific composite parameter ψ' the 'known' values used for the simulation were five evenly spaced points along the rank order of the estimates across the 106 genes. The MLE estimate for a given replicate were taken as the fit with the highest log-likelihood after running five independent analyses with different sets of naive starting points with respect to the composite ψ'_g parameter, α_c, and α_p. All analyses were carried out in our `selac` R package.

Analysis of yeast genomes & tests of model adequacy

We focus our empirical analyses on the large yeast data set and phylogeny of Salichos and Rokas (2013). As a model system, the yeast genome is an ideal system to examine our phylogenetic estimates of gene expression and its connection to real world measurements of these data within individual taxa. The complete data set of Salichos and Rokas (2013) contain 1070 orthologs, where we selected 100 at random for our analyses. We also focus our analyses on *Saccharomyces sensu stricto* and their sister taxon *Candida glabrata*, and we used the phylogeny depicted in Fig. 1 of Salichos and Rokas (2013) for our fixed tree. We fit the two SelAC models described above (i.e., SelAC and SelAC+Γ), as well as two codon models, GY and FMutSel, and a standard GTR + Γ nucleotide model. The FMutSel model assumes that the amino acid frequencies are determined by functional requirements of the protein while the other models make no assumptions about amino acid frequencies. In all cases, we assumed that the model was partitioned by gene, but with branch lengths linked across genes.

We also compared SelAC models with 195 codon models in IQtree (Nguyen *et al.*, 2015). This is popular software implementing various (i.e., Goldman and Yang (1994); Kosiol *et al.* (2007); Muse and Gaut (1994); Schneider *et al.* (2005)) models of evolution, including codon models. Most analyses within a set of software tools focus on differences in log-likelihood values between models. As a result, some software tools sometimes fail to include soley data dependent terms, which function as constants, in their calculations. Failure to include these terms can model comparison between software packages problematic. For simplicity, no constants are dropped in the log-likelihood calculations for SelAC. Further, while there are no identical models in SelAC and IQtree, similar models have similar likelihoods, suggesting the log-likelihood values between SelAC and IQtree are comparable. We note, however, that minor differences in

model implementation can lead to small differences in log likelihood (for example, how missing data is handled, as SelAC treats it as an absence at that site for that taxon, while some other software integrates across all possible states).

For SelAC, we compared our estimates of $\phi' = \psi'/\mathbf{B}$, which represents the average protein synthesis rate of a gene, to estimates of gene expression from empirical data. Specifically, we examined gene expression data for five of the six species measured during log-growth phase. Gene expression in this context corresponds to mRNA abundances, which were measured using either microarrays (*C. glabrata* and *S. castellii*, or RNA-Seq (*S. paradoxus*, *S. mikatae*, and *S. cerevisiae*). We obtained expression data for the remaining species, *S. kudriavzevii*, which was measured at the beginning of the stationary phase from the Gene Expression Omnibus (GEO). Saccharomyces, however, only enter the stationary growth phase in response to severe stress, such as starvation. In addition, only 56 % of the genes examined with SelAC had expression measurements available. For these reasons, we excluded *S. kudriavzevii* from our comparisons of empirical gene expression.

For further comparison, we also predicted the average protein synthesis rate for each gene ϕ by analyzing gene and genome-wide patterns of synonymous codon usage using ROC-SEMPPR (Gilchrist *et al.*, 2015) for each individual genome. While, like SelAC, ROC-SEMPPR uses codon level information, it does not rely on any interspecific comparisons and, unlike SelAC, uses only the intra- and inter-genic frequencies of synonymous codon usage as its data. Nevertheless, ROC-SEMPPR predictions of gene expression ϕ correlates strongly (Pearson $r = 0.53 - 0.74$) with a wide range of laboratory measurements of gene expression (Gilchrist *et al.*, 2015).

While one of our main objectives was to determine the improvement of fit that SelAC has with respect to other standard phylogenetic models, we also evaluated the adequacy of SelAC. Model fit, measured with assessments such as the Akaike Information Criterion (AIC), can tell which model is least bad as an approximation for the data, but it does not reveal whether a model is actually doing a good job of representing the data. An adequate model does the latter, one measure of which is that data generated under the model resemble real data (Goldman, 1993). For example, Beaulieu *et al.* (2013) assessed whether parsimony scores and the size of monomorphic clades of empirical data were within the distributions of simulated data under a new model and the best standard model; if the empirical summaries were outside the range for each, it would have suggested that neither model was adequately modeling this part of the biology.

In order to test adequacy for a given gene we first remove a particular taxon from the data set and the phylogeny. A marginal reconstruction of the likeliest sequence across all remaining nodes is

703 conducted under the model, including the node where the pruned taxon attached to the tree. The

704 marginal probabilities of each site are used to sample and assemble the starting coding sequence. This

705 sequence is then evolved along the branch, periodically being sampled and its current functionality

706 assessed. We repeat this process 100 times and compare the distribution of trajectories against the

707 observed functionality calculated for the gene. For comparison, we also conducted the same test, by

708 simulating the sequence under the standard GTR $+$ Γ nucleotide model, which is often used on these

709 data but does not account for the fact that the sequences are protein coding, and under FMutSel, which

710 includes selection on codons but in a fundamentally different way as our model.

The appropriate estimator of bias for AIC

712 As part of the model set described above, we also included a reduced form of each of the two SelAC

713 models, SelAC and SelAC+Γ. Specifically, rather than optimizing the amino acid at any given site, we

714 assume the the most frequently observed amino acid at each site is the optimal amino acid a^*. We refer to

715 these 'majority rule' models as SelAC$_M$ and SelAC$_M$+Γ and note that these majority rule formulations

716 greatly accelerate model fitting.

717 Since these majority rule models assume that the optimal amino acids are known prior to fitting of

718 our model, it is tempting to reduce the count of estimated parameters in the model by the number of

719 parameters estimated using majority rule. While using majority rule does not necessarily provide the

720 most likely parameter estimate, it nevertheless uses the data to generate the estimate and represents

721 a parameter estimated from the data. Thus, despite having become standard behavior in the field

722 of phylogenetics, this reduction is statistically inappropriate. Because the difference in the number of

723 parameters K when counting or not counting the number of nucleotide sites drops out when comparing

724 nucleotide models with AIC, this statistical issue does not apply to nucleotide models. It does, however,

725 matter for AICc, where K and the sample size n combine in the penalty term. This also matters in our

726 case, where the number of estimated parameters for the majority rule estimation differs based on whether

727 one is looking at codons or single nucleotides.

728 In phylogenetics two variants of AICc are used. In comparative methods (e.g. Beaulieu *et al.*, 2013;

729 Butler and King, 2004; O'Meara *et al.*, 2006) the number of data points, n, is taken as the number of

730 taxa. More taxa allow the fitting of more complex models, given more data. However, in DNA evolution,

731 which is effectively the same as a discrete character model used in comparative methods, the n is taken

732 as the number of sites. Obviously, both cannot be correct. This uncertainty was highlighted by Posada

733 and Buckley (2004): they chose to use number of sites, but mentioned in their discussion that sample size

734 also depends on the number of taxa. Sullivan and Joyce (2005) also mention that while the number of

24

735   sites is often taken as sample size, whether that is appropriate in phylogenetics is not entirely clear. One

736   approach incorporating both number of taxa and sites in calculating AICc is the program SURFACE

737   implemented by Ingram and Mahler (2013), which uses multiple characters and taxa. While its default

738   is to use AIC to compare models, if one chooses to use AICc, the number of samples is taken as the

739   product of number of sites and number of taxa.

740   Recently, Jhwueng *et al.* (2014) performed an analysis that investigated what variant of AIC and AICc

741   worked best as an estimator, but the results were inconclusive. Here, we have adopted and extended the

742   simulation approach of Jhwueng *et al.* (2014) in order to examine a large set of different penalty functions

743   and how well they approximate the remaining portion of the Kullback-Liebler (KL) divergence between

744   two models after accounting for the deviance (i.e., $-2\mathcal{L}$) (see Appendix 1 for more details).

Acknowledgements

References

Allison, S. 2012. A trait-based approach for modelling microbial litter decomposition. *Ecology Letters*, 15: 1058–1070.

Allison, S. and Goulden, M. 2017. Consequences of drought tolerance traits for microbial decompositionin the dement model. *Soil Biology & Biochemistry*, 107: 104–113.

Anisimova, M. 2012. Parametric models of codon evolution. In G. M. Cannarozzi and A. Schneider, editors, *Codon Evolution: Mechanisms and Models*, pages 12–33. Oxford University Press, Oxford, UK.

Asimov, I. 1989. The relativity of wrong. *The Skeptical Inquirer*, 14(1): 35–44.

Beaulieu, J. M. and O'Meara, B. C. 2016. Detecting hidden diversification shifts in models of trait-dependent speciation and extinction. *Systematic Biology*, 65(4): 583–601.

Beaulieu, J. M., O'Meara, B. C., and Donoghue, M. J. 2013. Identifying hidden rate changes in the evolution of a binary morphological character: The evolution of plant habit in campanulid angiosperms. *Systematic Biology*, 62(5): 725–737.

Berg, J. and Lässig, M. 2003. Stochastic evolution and transcription factor binding sites. *Biophysics*, 48(S1): S36–S44.

Blazej, P., Mackiewicz, D., Grabinska, M., Wnetrzak, M., and Mackiewicz, P. 2017. Optimization of amino acid replacement costs by mutational pressure in bacterial genomes. *Scientific Reports*, 7(1): 1061.

Box, G. E. P. 1976. Science and statistics. *Journal of the American Statistical Association*, 71(356): 791–799.

Brown, L. and Elliot, T. 1997. Mutations that increase expression of the rpos gene and decrease its dependence on hfq function in salmonella typhimurium. *J. Bacteriol.*, 179(3): 656–662.

Butler, M. A. and King, A. A. 2004. Phylogenetic comparative analysis: a modeling approach for adaptive evolution. *American Naturalist*, 164(6): 683–695.

Dimmic, M. W., Mindell, D. P., and Goldstein, R. A. 2000. Modeling evolution at the protein level using an adjustable amino acid fitness model. *Pacific Symposium on Biocomputing*, 5: 18–29.

Drummond, D. A. and Wilke, C. O. 2008. Mistranslation-induced protein misfolding as a dominant constraint on coding-sequence evolution. *Cell*, 134: 341–352.

Drummond, D. A., Bloom, J. D., Adami, C., Wilke, C. O., and Arnold, F. H. 2005. Why highly expressed proteins evolve slowly. *Proceedings of the National Academy of Sciences of the United States of America*, 102(40): 14338–14343.

Drummond, D. A., Raval, A., and Wilke, C. O. 2006. A single determinant dominates the rate of yeast protein evolution. *Molecular Biology and Evolution*, 23(2): 327–337.

Edwards, A. 1984. *Likelihood*. Cambridge science classics. Cambridge University Press.

Endler, J. A. 1986. *Natural Selection in the Wild*, pages 16–17. Number 21 in Monographs in Population Biology. Princeton University Press, Princeton, NJ. reference for definition of diversifying selection.

Felsenstein, J. 1981. Evolutionary trees from DNA-sequences - a maximum-likelihood approach. *Journal of Molecular Evolution*, 17: 368–376.

Felsenstein, J. 2001. Taking variation of evolutionary rates between sites into account in inferring phylogenies. *Journal of Molecular Evolution*, 53(4): 447–455.

Fisher, Ronald A., S. 1930. *The Genetical Theory of Natural Selection*. Oxford University Press, Oxford.

Gilchrist, M., Shah, P., and Zaretzki, R. 2009. Measuring and detecting molecular adaptation in codon usage against nonsense errors during protein translation. *Genetics*, 183: 1493–1505.

Gilchrist, M. A. 2007. Combining models of protein translation and population genetics to predict protein production rates from codon usage patterns. *Molecular Biology and Evolution*, 24: 2362–2373.

Gilchrist, M. A. and Wagner, A. 2006. A model of protein translation including codon bias, nonsense errors, and ribosome recycling. *Journal of Theoretical Biology*, 239: 417–434.

Gilchrist, M. A., Chen, W.-C., Shah, P., Landerer, C. L., and Zaretzki, R. 2015. Estimating gene expression and codon-specific translational efficiencies, mutation biases, and selection coefficients from genomic data alone. *Genome Biology and Evolution*, 7(6): 1559–1579.

Goldman, N. 1993. Statistical tests of models of dna substitution. *Journal of molecular evolution*, 36(2): 182–198.

Goldman, N. and Yang, Z. H. 1994. Codon-based model of nucleotide substitution for protein-coding DNA-sequences. *Molecular Biology and Evolution*, 11: 725–736.

Goldman, N., Thorne, J. L., and Jones, D. T. 1996. Using evolutionary trees in protein secondary structure prediction and other comparative sequence analyses. *Journal of Molecular Biology*, 263(2): 196 – 208.

Goldman, N., Thorne, J. L., and Jones, D. T. 1998. Assessing the impact of secondary structure and solvent accessibility on protein evolution. *Genetics*, 149(1): 445–458.

Goldsmith, M. and Tawfik, D. S. 2009. Potential role of phenotypic mutations in the evolution of protein expression and stability. *Proceedings of the National Academy of Sciences*, 106(15): 6197–6202.

Grantham, R. 1974. Amino acid difference formula to help explain protein evolution. *Science*, 185(4154): 862–864.

Halpern, A. L. and Bruno, W. J. 1998. Evolutionary distances for protein-coding sequences: Modeling site-specific residue frequencies. *Molecular Biology And Evolution*, 15: 910–917.

Higgs, P. G. 2008. Linking population genetics to phylogenetics. *Banach Center Publications*, 80(1): 145–166.

Hoehna, S., Landis, M. J., Heath, T. A., Boussau, B., Lartillot, N., Moore, B. R., Huelsenbeck, J. P., and Ronquist, F. 2016. Revbayes: Bayesian phylogenetic inference using graphical models and an interactive model-specification language. *Systematic Biology*, 65(4): 726.

Hughes, A. L. 2007. Looking for darwin in all the wrong places: the misguided quest for positive selection at the nucleotide sequence level. *Heredity*, 99: 364–373.

Hughes, A. L. and Nei, M. 1988. Pattern of nucleotide substitution at major histocompatibility complex class-i loci reveals overdominant selection. *Nature*, 335: 167–170.

Hughes, A. L., Ota, T., and Nei, M. 1990. Positive darwinian selection promotes charge profile diversity in the antigen-binding cleft of class-i major-histocompatibility-complex molecules. *Molecular Biology And Evolution*, 7: 515–524.

Ingram, T. and Mahler, D. L. 2013. Surface: detecting convergent evolution from data by fitting ornstein-uhlenbeck models with stepwise akaike information criterion. *Methods in ecology and evolution*, 4(5): 416–425.

Iwasa, Y. 1988. Free fitness that always increases in evolution. *Journal of Theoretical Biology*, 135: 265–281.

Jhwueng, D.-C., Snehalata, H., O'Meara, B. C., and Liu, L. 2014. Investigating the performance of aic in selecting phylogenetic models. *Statistical applications in genetics and moleculr biology*, 13(4): 459–475.

Johnson, S. G. 2012. *The NLopt nonlinear-optimization package*. Version 2.4.2 – Released 20 May 2014.

Kimura, M. 1962. on the probability of fixation of mutant genes in a population. *Genetics*, 47(6): 713–719.

King, Z. A., Lloyd, C. J., Feist, A. M., and Palsson, B. O. 2015. Next-generation genome-scale models for metabolic engineering. *Current Opinion in Biotechnology*, 35: 23 – 29.

Koshi, J. M. and Goldstein, R. A. 1997. Mutation matrices and physical-chemical properties: Correlations and implications. *Proteins-Structure Function And Genetics*, 27: 336–344.

Koshi, J. M. and Goldstein, R. A. 2000. Analyzing site heterogeneity during protein evolution. In *Biocomputing 2001*, pages 191–202. World Scientific.

Koshi, J. M., Mindell, D. P., and Goldstein, R. A. 1999. Using physical-chemistry-based substitution models in phylogenetic analyses of hiv-1 subtypes. *Molecular biology and evolution*, 16: 173–179.

Kosiol, C., Holmes, I., and Goldman, N. 2007. An empirical codon model for protein sequence evolution. *Molecular Biology and Evolution*, 24(7): 1464–1479.

Kubatko, L., Shah, P., Herbei, R., and Gilchrist, M. A. 2016. A codon model of nucleotide substitution with selection on synonymous codon usage. *Molecular Phylogenetics and Evolution*, 94(Part A): 290 – 297.

Lartillot, N. and Philippe, H. 2004. A bayesian mixture model for across-site heterogeneities in the amino-acid replacement process. *Molecular Biology And Evolution*, 21: 1095–1109.

Lerman, J. A., Hyduke, D. R., Latif, H., Portnoy, V. A., Lewis, N. E., Orth, J. D., Schrimpe-Rutledge, A. C., Smith, R. D., Adkins, J. N., Zengler, K., and Palsson, B. O. 2012. In silico method for modelling metabolism and gene product expression at genome scale. *Nature Communications*, 3: 929 EP –. Article.

Lynch, M. and Marinov, G. K. 2015. The bioenergetic costs of a gene. *Proceedings Of The National Academy Of Sciences Of The United States Of America*, 112: 15690–15695.

Mayrose, I., Friedman, N., and Pupko, T. 2005. A gamma mixture model better accounts for among site rate heterogeneity. *Bioinformatics*, 21(suppl-2): ii151–ii158.

McCandlish, D. M. and Stoltzfus, A. 2014. Modeling evolution using the probability of fixation: History and implications. *The Quarterly Review of Biology*, 89(3): 225–252.

McClellan, D. A. and McCracken, K. G. 2001. Estimating the influence of selection on the variable amino acid sites of the cytochrome b protein functional domains. *Molecular Biology And Evolution*, 18: 917–925.

Muse, S. V. and Gaut, B. S. 1994. A likelihood approach for comparing synonymous and nonsynonymous nucleotide substitution rates, with application to the chloroplast genome. *Molecular Biology and Evolution*, 11(5): 715–724.

Nguyen, L.-T., Schmidt, H. A., von Haeseler, A., and Minh, B. Q. 2015. Iq-tree: A fast and effective stochastic algorithm for estimating maximum-likelihood phylogenies. *Molecular Biology and Evolution*, 32(1): 268–274.

Nielsen, R. and Yang, Z. H. 1998. Likelihood models for detecting positively selected amino acid sites and applications to the hiv-1 envelope gene. *Genetics*, 148: 929–936.

Nowak, M. A. 2006. *Evolutionary Dynamics: Exploring the Equations of Life*. Belknap of Harvard University Press, Cambridge, MA.

O'Meara, B. C., Ane, C., Sanderson, M. J., and P.C., W. 2006. Testing for different rates of continuous trait evolution using likelihood. *Evolution*, 60(5): 922–933.

Pellmyr, O. 2002. Microevolution. In M. Pagel, editor, *Encyclopedia of Evolution*, volume 2, pages 731–732. Oxford University Press, Oxford, UK.

Penny, D., McComish, B. J., Charleston, M. A., and Hendy, M. D. 2001. Mathematical elegance with biochemical realism: The covarion model of molecular evolution. *Journal Of Molecular Evolution*, 53: 711–723.

Pollock, D. D., Thiltgen, G., and Goldstein, R. A. 2012. Amino acid coevolution induces an evolutionary stokes shift. *Proceedings Of The National Academy Of Sciences Of The United States Of America*, 109: E1352–E1359.

Posada, D. and Buckley, T. R. 2004. Model selection and model averaging in phylogenetics: advantages of akaike information criterion and bayesian approaches over likelihood ratio tests. *Systematic Biology*, 53(5): 793–808.

Pouyet, F., Bailly-Bechet, M., Mouchiroud, D., and Guguen, L. 2016. Senca: A multilayered codon model to study the origins and dynamics of codon usage. *Genome Biology and Evolution*, 8(8): 2427–2441.

Rabosky, D. L. and Goldberg, E. E. 2015. Model inadequacy and mistaken inferences of trait-dependent speciation. *Systematic Biology*, 64(2): 340–355.

Robinson, D. M., Jones, D. T., Kishino, H., Goldman, N., and Thorne, J. L. 2003. Protein evolution with dependence among codons due to tertiary structure. *Molecular Biology And Evolution*, 20: 1692–1704.

Rodrigue, N. and Lartillot, N. 2014. Site-heterogeneous mutation-selection models within the phylobayes-mpi package. *Bioinformatics*, 30: 1020–1021.

Rodrigue, N., Lartillot, N., Bryant, D., and Philippe, H. 2005. Site interdependence attributed to tertiary structure in amino acid sequence evolution. *Gene*, 347: 207–217.

Rokas, A., Williams, B. L., King, N., and Carroll, S. B. 2003. Genome-scale approaches to resolving incongruence in molecular phylogenies. *Nature*, 425: 798–804.

Rowan, T. 1990. *Functional Stability Analysis of Numerical Algorithms*. Ph.D. thesis, University of Texas, Austin.

Salichos, L. and Rokas, A. 2013. Inferring ancient divergences requires genes with strong phylogenetic signals. *Nature*, 497(7449): 327–331.

Schneider, E., Moore, M., and Castro, K. G. 2005. Epidemiology of tuberculosis in the united states. *Clinics in Chest Medicine*, 26: 183–+.

Sella, G. and Hirsh, A. E. 2005. The application of statistical physics to evolutionary biology. *Proceedings of the National Academy of Sciences of the United States of America*, 102: 9541–9546.

Shah, P. and Gilchrist, M. A. 2011. Explaining complex codon usage patterns with selection for translational efficiency, mutation bias, and genetic drift. *Proceedings of the National Academy of Sciences of the United States of America*, 108(25): 10231–10236.

Shah, P., McCandlish, D. M., and Plotkin, J. B. 2015. Contingency and entrenchment in protein evolution under purifying selection. *Proceedings of the National Academy of Sciences*, 112(25): E3226–E3235.

Stamatakis, A. 2006. RAxML-VI-HPC: maximum likelihood-based phylogenetic analyses with thousands of taxa and mixed models. *Bioinformatics*, 22(21): 2688–2690.

Sullivan, J. and Joyce, P. 2005. Model selection in phylogenetics. *Annual Review of Ecology, Evolution, and Systematics*, 36(1): 445–466.

Tamuri, A. U., dos Reis, M., Hay, A. J., and Goldstein, R. A. 2009. Identifying changes in selective constraints: Host shifts in influenza. *Plos Computational Biology*, 5.

Tamuri, A. U., dos Reis, M., and Goldstein, R. A. 2012. Estimating the distribution of selection coefficients from phylogenetic data using sitewise mutation-selection models. *Genetics*, 190: 1101–1115.

Tamuri, A. U., Goldman, N., and dos Reis, M. 2014. A penalized-likelihood method to estimate the distribution of selection coefficients from phylogenetic data. *Genetics*, 197: 257–271.

Thiele, I., Fleming, R. M. T., Que, R., Bordbar, A., Diep, D., and Palsson, B. O. 2012. Multiscale modeling of metabolism and macromolecular synthesis in e. coli and its application to the evolution of codon usage. *PLOS ONE*, 7(9): 1–18.

Thorne, J. L., Goldman, N., and Jones, D. T. 1996. Combining protein evolution and secondary structure. *Molecular Biology and Evolution*, 13(5): 666–673.

Thorne, J. L., Lartillot, N., Rodrigue, N., and Choi, S. C. 2012. Codon models as a vehicle for reconciling population genetics with inter-specific sequence data. *Codon Evolution: Mechanisms And Models*, pages 97–110 D2 10.1093/acprof:osobl/9780199601165.001.0001 ER.

Tuffley, C. and Steel, M. 1998. Modeling the covarion hypothesis of nucleotide substitution. *Mathematical Biosciences*, 147: 63–91.

Wagner, A. 2005. Energy constraints on the evolution of gene expression. *Molecular Biology and Evolution*, 22: 1365–1374.

Whelan, S. 2008. Spatial and temporal heterogeneity in nucleotide sequence evolution. *Molecular Biology And Evolution*, 25: 1683–1694.

Whelan, S. and Goldman, N. 2004. Estimating the frequency of events that cause multiple-nucleotide changes. *Genetics*, 167(4): 2027–2043.

Woolley, S., Johnson, J., Smith, M. J., Crandall, K. A., and McClellan, D. A. 2003. Treesaap: Selection on amino acid properties using phylogenetic trees. *Bioinformatics*, 19(5): 671–672.

Wright, S. 1969. *Evolution and the genetics of populations. Vol. 2. The theory of gene frequencies.*, volume 2. University of Chicago Press.

Xia, X. H. and Li, W. H. 1998. What amino acid properties affect protein evolution? *Journal Of Molecular Evolution*, 47: 557–564.

Yang, Z. 2014. *Molecular Evolution: A Statistical Approach*. Oxford University Press, New York.

Yang, Z., Nielsen, R., and Hasegawa, M. 1998. Models of amino acid substitution and applications to mitochondrial protein evolution. *Molecular Biology and Evolution*, 15: 1600–1611.

Yang, Z. H. 1994. Maximum-likelihood phylogenetic estimation from DNA-sequences with variable rates over sites - approximate methods. *Journal Of Molecular Evolution*, 39: 306–314.

Yang, Z. H. 2007. Paml 4: Phylogenetic analysis by maximum likelihood. *Molecular Biology And Evolution*, 24: 1586–1591.

Yang, Z. H. and Nielsen, R. 1998. Synonymous and nonsynonymous rate variation in nuclear genes of mammals. *Journal Of Molecular Evolution*, 46: 409–418.

Yang, Z. H. and Nielsen, R. 2008. Mutation-selection models of codon substitution and their use to estimate selective strengths on codon usage. *Molecular Biology and Evolution*, 25: 568–579.

Zanger, U. and Schwab, M. 2013. Cytochrome p450 enzymes in drug metabolism: Regulation of gene expression, enzyme activities, and impact of genetic variation. *Pharmacology & Therapeutics*, 138: 103–141.

935 **Table**

| | Parameters | | | | Model |
Model	$-\ln(\mathcal{L})$	Estimated	AIC	AICc	ΔAICc	Weight
SelAC+Γ	453,620.8	50,005	1,007,252	1,027,314	0	>0.999
SelAC	464,114.8	50,004	1,028,238	1,048,299	20,985	<0.001
SelAC$_M$+Γ	465,106.9	50,005	1,030,224	1,050,286	22,972	<0.001
SelAC$_M$	478,302.4	50,004	1,056,613	1,076,674	49,360	<0.001
FMutSel	597,140.7	178	1,194,637	1,194,638	167,324	<0.001
GY	612,670.4	111	1,225,563	1,225,563	198,249	<0.001
GTR+Γ	655,166.4	610	1,311,553	1,311,554	284,240	<0.001

Table 1. Comparison of maximum likelihood fits for SelAC and commonly used models based on negative log likelihood ($-ln(\mathcal{L})$), AIC, AICc, and AIC$_W$ from analyses of 100 selected genes from 6 yeast taxa Salichos and Rokas (2013). Note the subscripts M indicate model fits where the most common or 'majority rule' amino acid was fixed as the optimal amino acid a^* for each site. As discussed in text, despite the fact that a^* for each site under M was not fitted by our algorithm, its value was determined by examining the data and, as a result, represent an additional parameter estimated from the data and are accounted for in our table. Sample size used in the calculation of AICc is assumed to be equal to the size of the matrix (number of taxa x number of sites $= 6 \times 49,881 = 299,286$). For the comparison between the different SelAC and 192 other models fitted using IQTree (Nguyen *et al.*, 2015) see Table S1 in the Supporting Materials. In summary, the different SelAC models and FMutSel fitted the data better than any of the IQTree models.

936 **Figures**
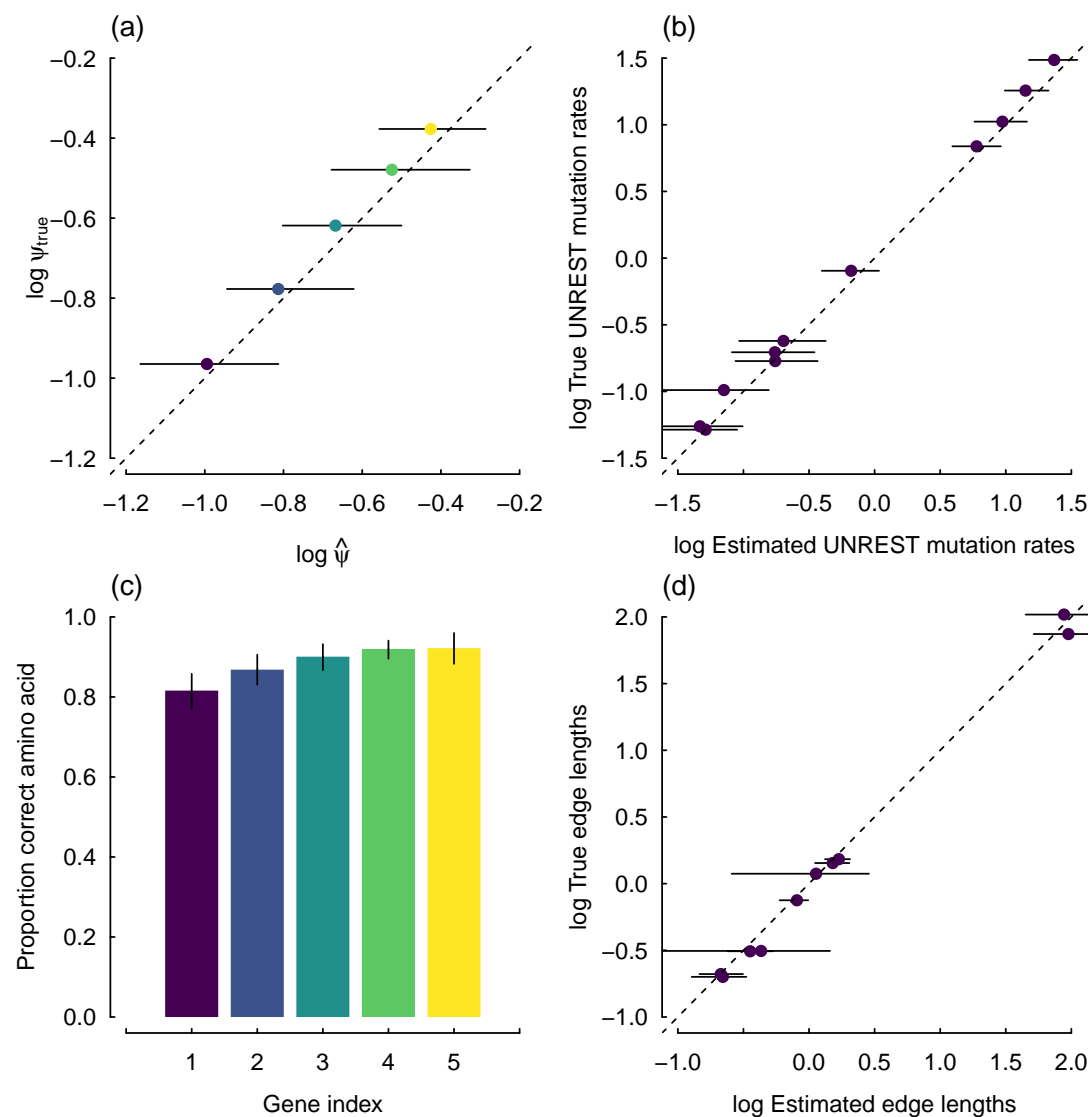
FIG. 1. Summary of a 5-gene simulation for a SelAC model where we assume $\alpha_G = \infty$, and thus, no site-specific sensitivity in the generating model. The 'known' parameters were based on fitting the SelAC model to the 106 gene data set and phylogeny of Rokas *et al.* (2003), with gene choice being based on five evenly spaced points along the rank order of the

gene specific composite parameter ψ'_g. The points and associated uncertainty in the estimates of the gene-specific average

protein synthesis rate, or ψ (calculated from ψ')(a), nucleotide mutation rates under the UNREST model (b), proportion of correct optimal amino acids for a given gene (c), and estimates of the individual edge lengths are based the mean and 2.5% and 97.5% quantiles across all 50 simulated datasets (d). Gene index on the x-axis refers to the arbitrary number assigned to the simulated gene.
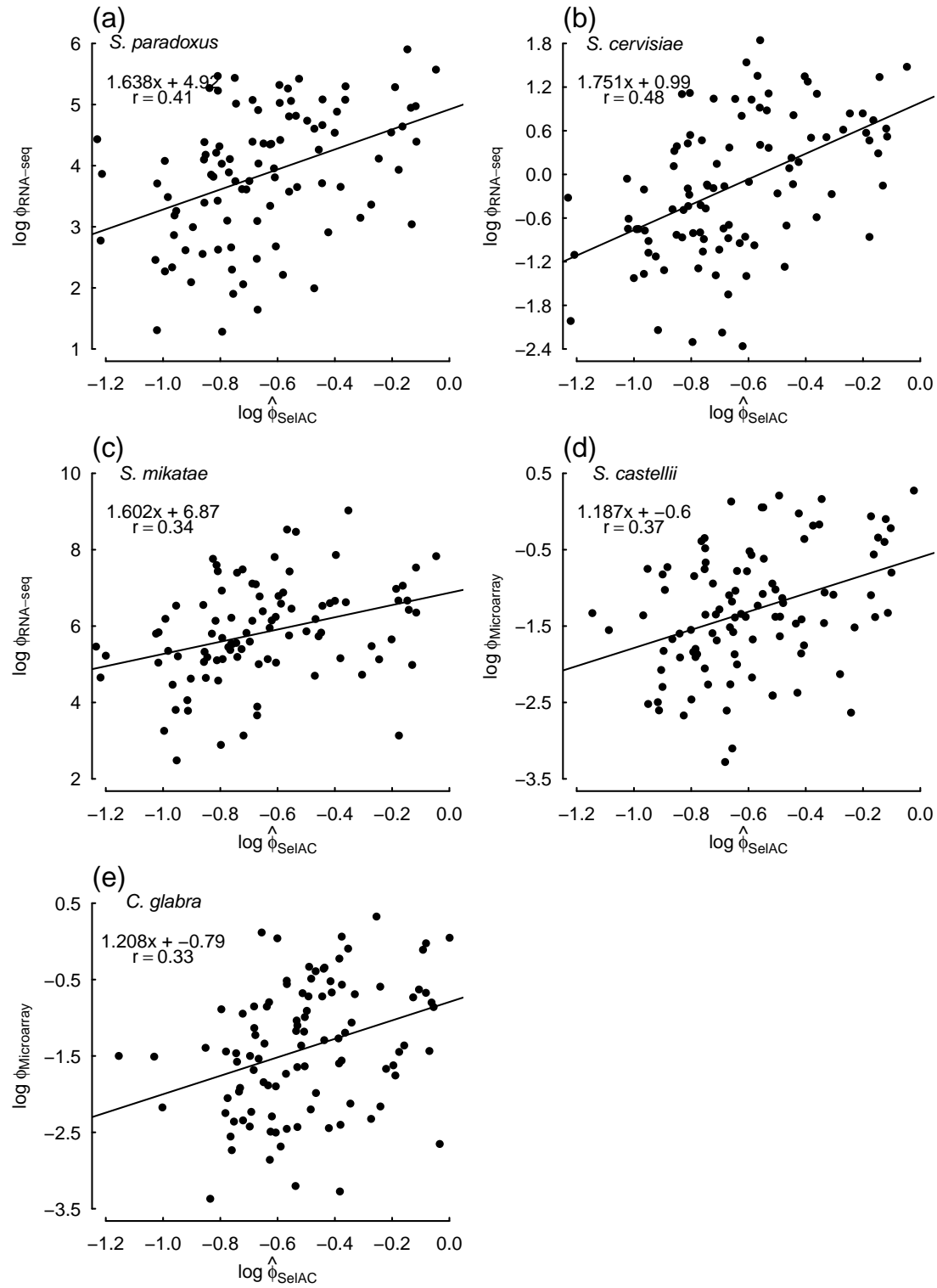
FIG. 2. Comparisons between estimates of average protein translation rate $\hat{\phi}_{\text{SelAC}}$ obtained from SelAC+Γ and direct measurements of expression for individual yeast taxa across the 100 selected genes from Salichos and Rokas (2013) measured during log-growth phase. Estimates of $\hat{\phi}_{\text{SelAC}}$ were generated by dividing the composite term ψ' by $\mathbf{B}(\vec{a}_i|\vec{a}^*)$. Gene expression was measured using either RNA-Seq (a)-(c) or microarray (d)-(e). The equations in the upper left hand corner of each panel represent the regression fit and the Pearson correlation coefficient r.
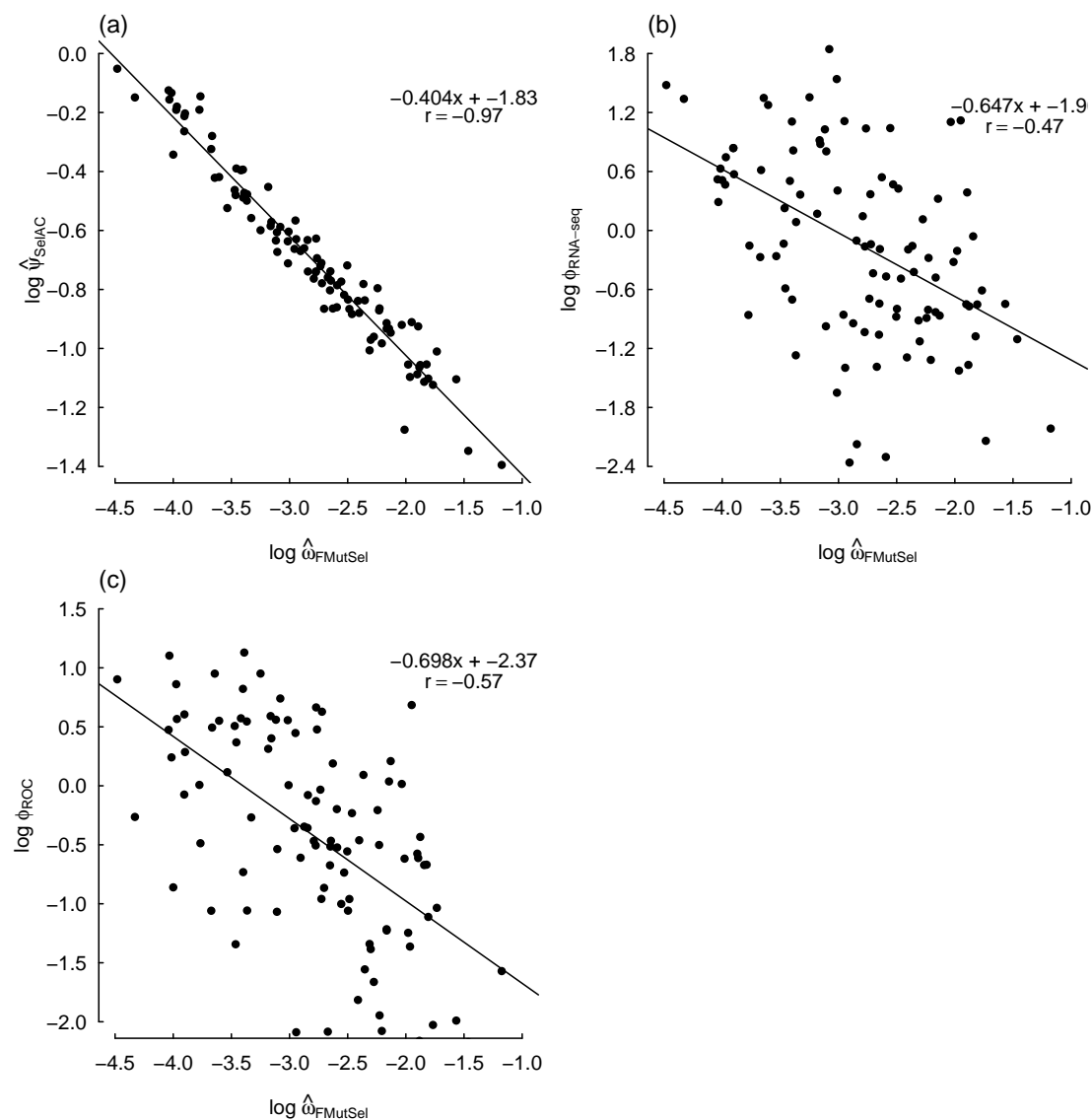
FIG. 3. Comparisons between ω_{FMutSel}, which is the nonsynonymous/synonymous mutation ratio in FMutSel, SelAC+Γ estimates of protein functionality production rates $\hat{\psi}_{\text{SelAC}}$ (a), RNA-Seq based measurements of mRNA abundance $\phi_{\text{RNA-seq}}$ (b), and ROC-SEMPPER's estimates of protein translation rates ϕ_{ROC}, which are based solely on *S. cerevisiae*'s patterns of codon usage bias (c), for *S. cerevisiae* across the 100 selected genes from Salichos and Rokas (2013). As in Figure 2, the equations in the upper right hand corner of each panel provide the regression fit and correlation coefficient.
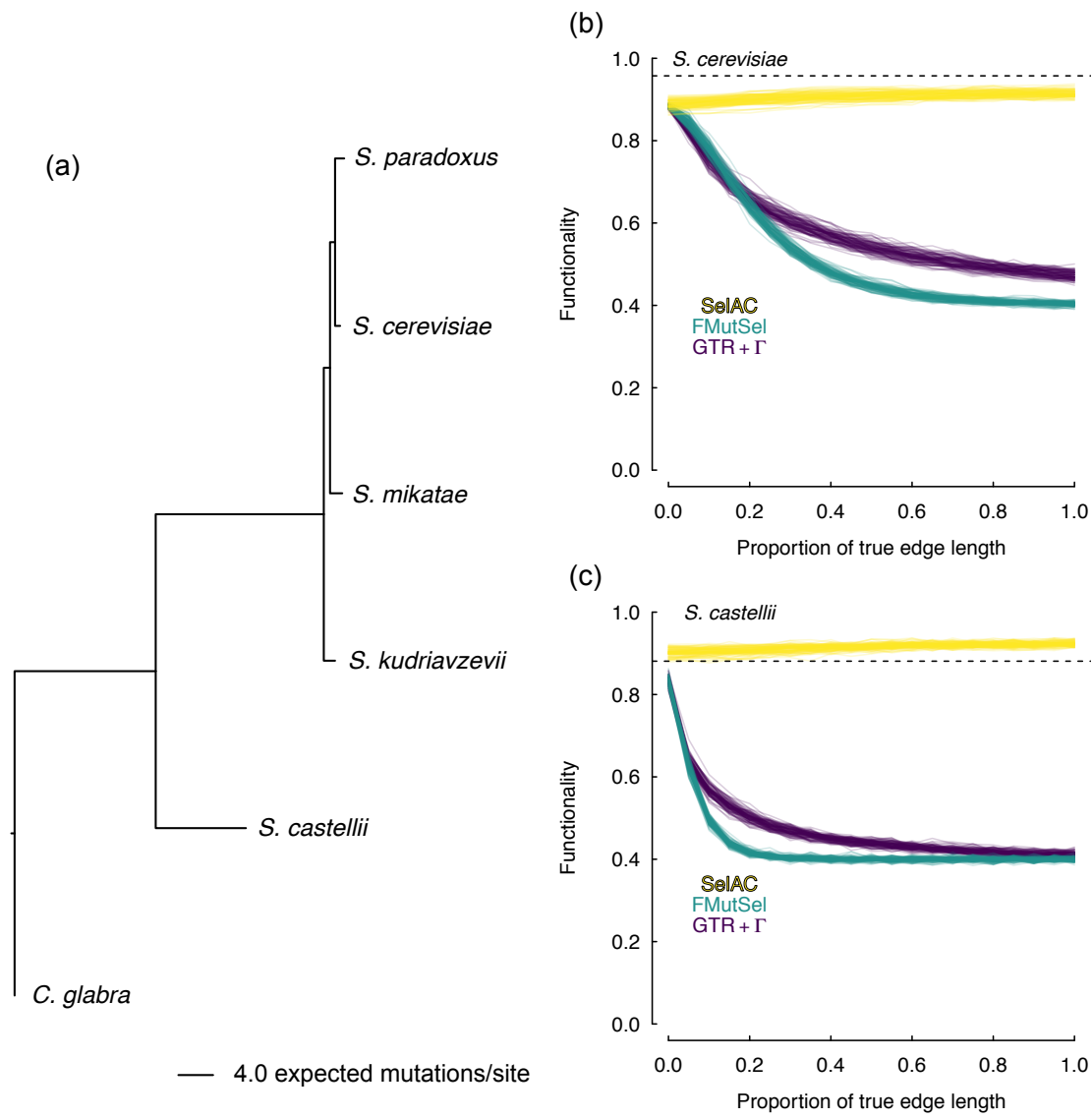
FIG. 4. (a) Maximum likelihood estimates of branch lengths under SelAC+Γ for 100 selected genes from Salichos and Rokas (2013). Tests of model adequacy for *S. cerevisiae* (b) and *S. castellii* (c) indicated that, when these taxa are removed from the tree, and their sequences are simulated, the parameters of SelAC+Γ exhibit functionality $\mathbf{B}(\vec{a}_{\mathrm{obs}}|\vec{a}^*)$ that is far closer to the observed (dashed black line) than data sets produced from parameters of either FMutSel or GTR + Γ.

Supporting Materials

Supporting Materials for *Population Genetics Based Phylogenetics Under Stabilizing Selection for an Optimal Amino Acid Sequence: A Nested Modeling Approach* by Beaulieu *et al.* (In Review).

Comparisons of SelAC gene expression estimates with empirical measurements

In our model, the parameter ϕ measures the realized average protein synthesis rate of a gene. We compared our estimates of ϕ to two separate measures of gene expression, one empirical (Figure S1), and one model-based prediction that does not account for shared ancestry, for individual yeast taxa across the same set of genes. Our estimates of ϕ are positively correlated with both measures, which are also reasonably well correlated with each other (Figure 2 - S2) On the whole, these comparisons indicate not only a high degree of consistency among all three measures, but also, importantly, that estimates of ϕ obtained from SelAC provide real biological insight into the expression level of a gene.
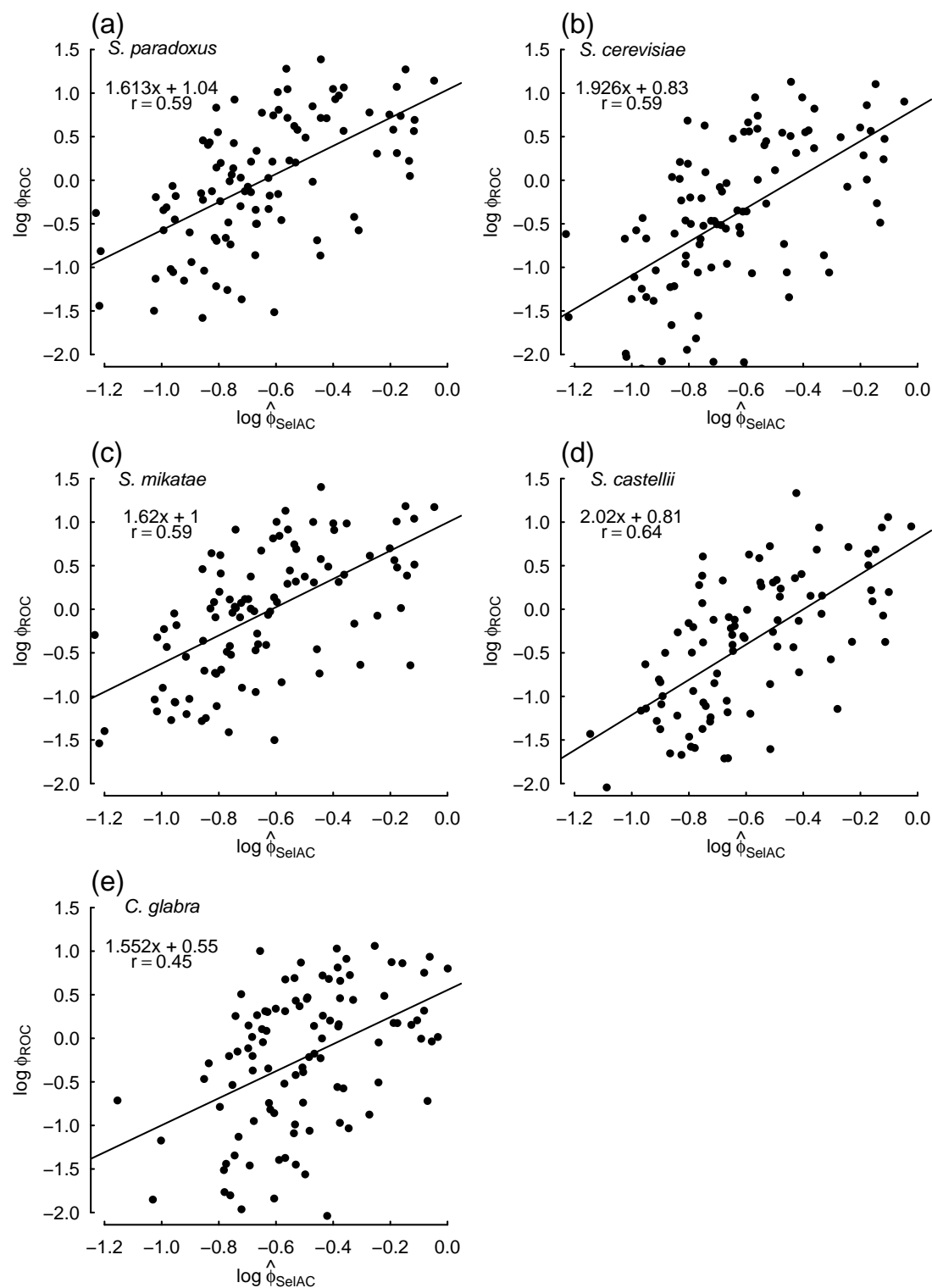
FIG. S1. Comparisons between estimates of ϕ obtained from SelAC+Γ and the predicted gene expression from the ROC SEMPER model (Gilchrist *et al.*, 2015) for individual yeast taxa across the 100 selected genes from Salichos and Rokas (2013). As with figures in the main text, estimates of ϕ were obtained by solving for ψ based on estimates of ψ', and then dividing by $\mathbf{B}(\vec{a}_i|\vec{a}^*)$. The equations in the upper left hand corner of each panel represent the regression fit and correlation coefficient.

FIG. S2. Comparisons of predicted gene expression from the ROC SEMPER model (Gilchrist *et al.* (2015)) and direct measurements of expression from RNA-Seq or microarray data for individual yeast taxa across the 100 selected genes from Salichos and Rokas (2013). The equations in the upper left hand corner of each panel represent the regression fit and correlation coefficient.

Table

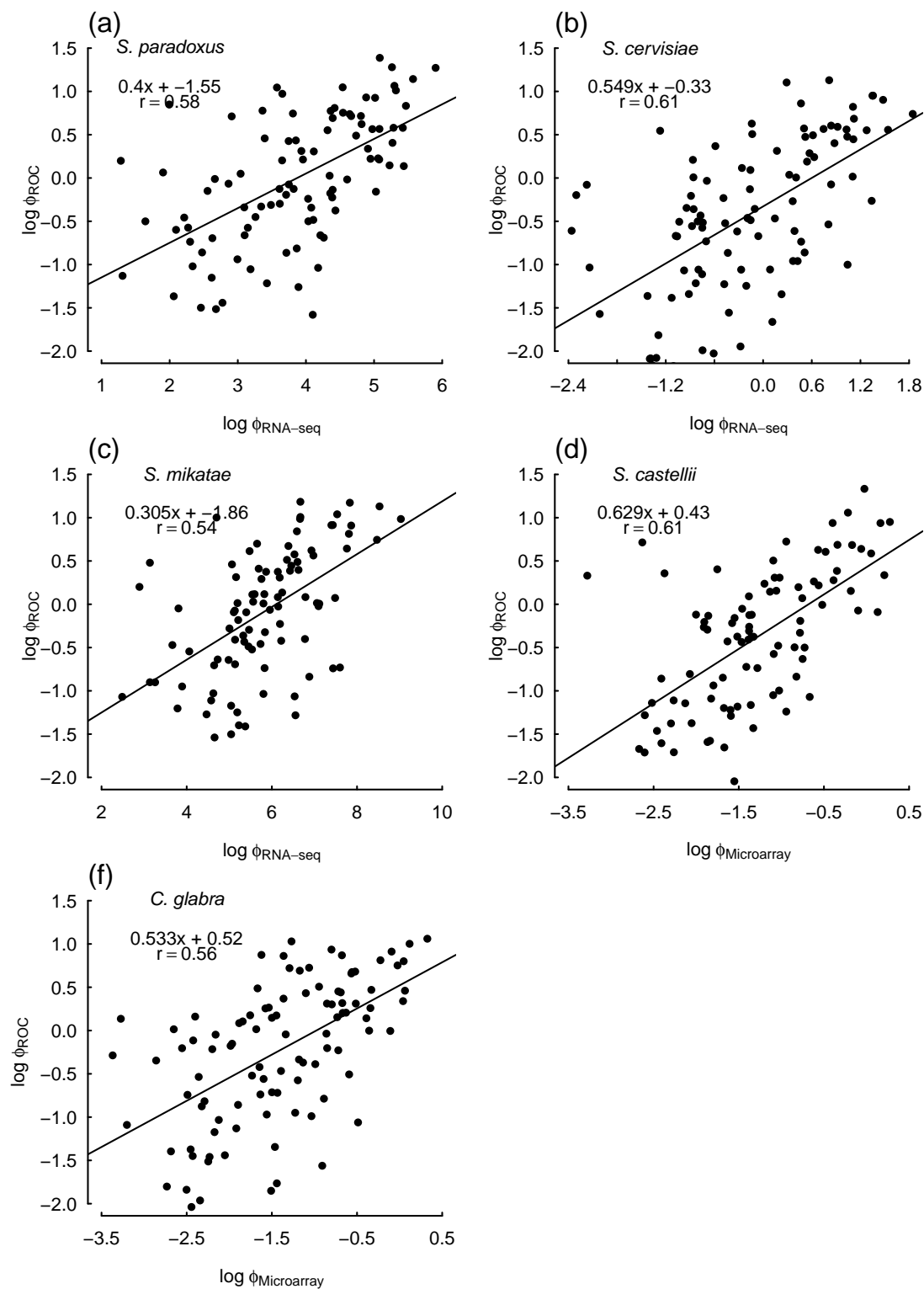Table S1.: Comparison of SelAC to 163 other phylogenetic models to 100 selected genes from 6 yeast taxa Salichos and Rokas (2013) using negative log likelihood ($-ln(\mathcal{L})$), AIC, and AICc values. See Table 1 for more details Models of Rank 1-4, 88, and 166 were fitted using the SelAC software package. All remaining models were fitted using IQTree (Nguyen *et al.*, 2015). Note that there are no models in common between IQTree and SelAC. SelAC's GY and IQTree's GY+F are the most similar. However, SelAC's GY uses a mutation model to generate expected codon frequencies while IQTree's GY+F uses the observed frequencies.

Rank	Model	$-\ln(\mathcal{L})$	df	AIC	AICc	ΔAIC	ΔAICc
1	SelAC+Γ	453,621	50,005	1,007,252	1,027,314	0	0
2	SelAC	464,115	50,004	1,028,238	1,050,286	20,986	22,972
3	SelAC$_M$+Γ	465,302	50,005	1,056,613	1,076,674	49,361	49,360
4	FMutSel	597,141	178	1,194,637	1,194,638	187,385	167,324
5	KOSI07+F+R10	598,031	87	1,196,235	1,196,236	188,983	168,922
6	KOSI07+F+R9	598,326	85	1,196,822	1,196,822	189,570	169,508
7	KOSI07+F+R8	598,609	83	1,197,383	1,197,384	190,131	170,070
8	KOSI07+F+R7	598,940	81	1,198,041	1,198,041	190,789	170,727
9	GY+F+R5	599,010	79	1,198,178	1,198,179	190,926	170,865
10	GY+F+R4	599,017	77	1,198,188	1,198,188	190,936	170,874
11	GY+F+R3	599,092	75	1,198,334	1,198,334	191,082	171,020
12	KOSI07+F+R6	599,337	79	1,198,832	1,198,832	191,580	171,518
13	GY+F+R2	599,662	73	1,199,471	1,199,471	192,219	172,157
14	KOSI07+F+R5	599,854	77	1,199,862	1,199,862	192,610	172,548
15	KOSI07+F+R4	600,572	75	1,201,293	1,201,294	194,041	173,980
16	GY+F+G4	600,946	72	1,202,037	1,202,037	194,785	174,723
17	GY+F+I+G4	600,947	73	1,202,040	1,202,040	194,788	174,726

Continued on next page

Table S1 – *Continued from previous page*

Rank	Model	$-\ln(\mathcal{L})$	df	AIC	AICc	ΔAIC	ΔAICc
18	SCHN05+F+R10	601,260	87	1,202,694	1,202,694	195,442	175,380
19	KOSI07+F+R3	601,538	73	1,203,222	1,203,222	195,970	175,908
20	SCHN05+F+R9	602,116	85	1,204,402	1,204,402	197,150	177,088
21	KOSI07+F+R2	603,128	71	1,206,397	1,206,397	199,145	179,083
22	SCHN05+F+R8	603,280	83	1,206,725	1,206,726	199,473	179,412
23	KOSI07+F+G4	604,152	70	1,208,444	1,208,445	201,192	181,131
24	KOSI07+F+I+G4	604,152	71	1,208,446	1,208,446	201,194	181,132
25	SCHN05+F+R7	604,739	81	1,209,639	1,209,639	202,387	182,325
26	KOSI07+F3X4+R9	605,979	34	1,212,026	1,212,026	204,774	184,712
27	MGK+F3X4+R5	606,033	28	1,212,121	1,212,121	204,869	184,807
28	MGK+F3X4+R4	606,037	26	1,212,127	1,212,127	204,875	184,813
29	MGK+F3X4+R3	606,057	24	1,212,163	1,212,163	204,911	184,849
30	GY+F3X4+R5	606,154	28	1,212,364	1,212,364	205,112	185,050
31	GY+F3X4+R6	606,153	30	1,212,365	1,212,365	205,113	185,051
32	GY+F3X4+R4	606,181	26	1,212,414	1,212,414	205,162	185,100
33	GY+F3X4+R3	606,212	24	1,212,472	1,212,472	205,220	185,158
34	SCHN05+F+R6	606,181	79	1,212,520	1,212,520	205,268	185,206
35	KOSI07+F3X4+R8	606,322	32	1,212,708	1,212,708	205,456	185,394
36	KOSI07+F3X4+R7	606,913	30	1,213,886	1,213,886	206,634	186,572
37	MGK+F3X4+R2	606,960	22	1,213,965	1,213,965	206,713	186,651
38	SCHN05+F3X4+R10	607,042	36	1,214,155	1,214,155	206,903	186,841
39	GY+F3X4+R2	607,143	22	1,214,329	1,214,329	207,077	187,015
40	SCHN05+F+R5	607,190	77	1,214,533	1,214,534	207,281	187,220
41	SCHN05+F3X4+R9	607,253	34	1,214,573	1,214,573	207,321	187,259
42	KOSI07+F3X4+R6	607,321	28	1,214,697	1,214,697	207,445	187,383
43	KOSI07+F3X4+R10	607,370	36	1,214,812	1,214,812	207,560	187,498
44	SCHN05+F3X4+R8	607,638	32	1,215,339	1,215,339	208,087	188,025
45	MGK+F3X4+G4	607,662	21	1,215,365	1,215,365	208,113	188,051

Table S1 – *Continued from previous page*

Rank	Model	$-\ln(\mathcal{L})$	df	AIC	AICc	ΔAIC	ΔAICc
46	MGK+F3X4+I+G4	607,663	22	1,215,370	1,215,370	208,118	188,056
47	GY+F+I	607,640	72	1,215,424	1,215,424	208,172	188,110
48	GY+F3X4+G4	607,743	21	1,215,527	1,215,527	208,275	188,213
49	GY+F3X4+I+G4	607,744	22	1,215,531	1,215,531	208,279	188,217
50	KOSI07+F3X4+R5	607,829	26	1,215,709	1,215,709	208,457	188,395
51	SCHN05+F+R4	607,792	75	1,215,734	1,215,735	208,482	188,421
52	SCHN05+F3X4+R7	608,418	30	1,216,897	1,216,897	209,645	189,583
53	SCHN05+F+R3	608,416	73	1,216,977	1,216,977	209,725	189,663
54	KOSI07+F3X4+R4	608,554	24	1,217,156	1,217,156	209,904	189,842
55	GY+F	608,565	71	1,217,273	1,217,273	210,021	189,959
56	GY+F1X4+R6	608,839	24	1,217,726	1,217,726	210,474	190,412
57	GY+F1X4+R5	608,842	22	1,217,728	1,217,728	210,476	190,414
58	GY+F1X4+R4	608,866	20	1,217,772	1,217,772	210,520	190,458
59	MGK+F1X4+R5	608,879	22	1,217,802	1,217,802	210,550	190,488
60	MGK+F1X4+R4	608,883	20	1,217,807	1,217,807	210,555	190,493
61	GY+F1X4+R3	608,889	18	1,217,813	1,217,813	210,561	190,499
62	MGK+F1X4+R3	608,907	18	1,217,851	1,217,851	210,599	190,537
63	SCHN05+F+R2	609,165	71	1,218,472	1,218,472	211,220	191,158
64	KOSI07+F3X4+R3	609,569	22	1,219,182	1,219,182	211,930	191,868
65	SCHN05+F3X4+R6	609,687	28	1,219,430	1,219,430	212,178	192,116
66	GY+F1X4+R2	609,813	16	1,219,659	1,219,659	212,407	192,345
67	MGK+F1X4+R2	609,820	16	1,219,672	1,219,672	212,420	192,358
68	SCHN05+F+G4	610,131	70	1,220,401	1,220,401	213,149	193,087
69	SCHN05+F+I+G4	610,131	71	1,220,403	1,220,403	213,151	193,089
70	GY+F1X4+G4	610,207	15	1,220,444	1,220,444	213,192	193,130
71	GY+F1X4+I+G4	610,208	16	1,220,447	1,220,447	213,195	193,133
72	MGK+F1X4+G4	610,273	15	1,220,575	1,220,575	213,323	193,261
73	MGK+F1X4+I+G4	610,274	16	1,220,580	1,220,580	213,328	193,266

Table S1 – *Continued from previous page*

Rank	Model	$-\ln(\mathcal{L})$	df	AIC	AICc	ΔAIC	ΔAICc
74	KOSI07+F+I	610,257	70	1,220,653	1,220,653	213,401	193,339
75	KOSI07+F1X4+R8	610,602	26	1,221,255	1,221,255	214,003	193,941
76	KOSI07+F	611,155	69	1,222,448	1,222,448	215,196	195,134
77	KOSI07+F1X4+R7	611,353	24	1,222,755	1,222,755	215,503	195,441
78	SCHN05+F3X4+R5	611,498	26	1,223,048	1,223,048	215,796	195,734
79	KOSI07+F1X4+R6	611,809	22	1,223,662	1,223,662	216,410	196,348
80	KOSI07+F3X4+R2	611,865	20	1,223,769	1,223,769	216,517	196,455
81	MG+F3X4+R7	612,290	31	1,224,642	1,224,642	217,390	197,328
82	MG+F3X4+R8	612,289	33	1,224,645	1,224,645	217,393	197,331
83	KOSI07+F1X4+R5	612,311	20	1,224,662	1,224,662	217,410	197,348
84	MG+F3X4+R6	612,313	29	1,224,683	1,224,683	217,431	197,369
85	MG+F3X4+R5	612,336	27	1,224,725	1,224,725	217,473	197,411
86	MG+F3X4+R4	612,355	25	1,224,760	1,224,760	217,508	197,446
87	MG+F3X4+R3	612,369	23	1,224,783	1,224,783	217,531	197,469
88	GY	612,670	111	1,225,563	1,225,563	218,311	198,249
89	KOSI07+F3X4+G4	612,932	19	1,225,903	1,225,903	218,651	198,589
90	KOSI07+F3X4+I+G4	612,932	20	1,225,905	1,225,905	218,653	198,591
91	SCHN05+F1X4+R10	612,982	30	1,226,024	1,226,024	218,772	198,710
92	KOSI07+F1X4+R4	612,995	18	1,226,025	1,226,026	218,773	198,712
93	MG+F3X4+R2	613,159	21	1,226,360	1,226,360	219,108	199,046
94	MGK+F3X4+I	613,206	21	1,226,454	1,226,454	219,202	199,140
95	KOSI07+F1X4+R9	613,259	28	1,226,574	1,226,574	219,322	199,260
96	SCHN05+F1X4+R9	613,320	28	1,226,696	1,226,696	219,444	199,382
97	SCHN05+F3X4+R4	613,713	24	1,227,474	1,227,474	220,222	200,160
98	SCHN05+F1X4+R8	613,817	26	1,227,686	1,227,686	220,434	200,372
99	MG+F3X4+G4	613,854	20	1,227,747	1,227,747	220,495	200,433
100	MG+F3X4+I+G4	613,856	21	1,227,753	1,227,753	220,501	200,439
101	KOSI07+FU+R6	614,272	19	1,228,581	1,228,581	221,329	201,267

Table S1 – *Continued from previous page*

Rank	Model	$-\ln(\mathcal{L})$	df	AIC	AICc	ΔAIC	ΔAICc
102	KOSI07+FU+R5	614,454	17	1,228,942	1,228,942	221,690	201,628
103	GY+F3X4+I	614,457	21	1,228,957	1,228,957	221,705	201,643
104	SCHN05+F1X4+R7	614,535	24	1,229,119	1,229,119	221,867	201,805
105	KOSI07+F1X4+R3	614,556	16	1,229,144	1,229,144	221,892	201,830
106	MGK+F3X4	614,642	20	1,229,325	1,229,325	222,073	202,011
107	KOSI07+FU+R7	614,772	21	1,229,586	1,229,586	222,334	202,272
108	SCHN05+F1X4+R6	615,584	22	1,231,212	1,231,212	223,960	203,898
109	MG+F1X4+R4	615,590	19	1,231,217	1,231,217	223,965	203,903
110	MG+F1X4+R3	615,596	17	1,231,225	1,231,225	223,973	203,911
111	MGK+F1X4+I	615,826	15	1,231,682	1,231,682	224,430	204,368
112	GY+F3X4	615,827	20	1,231,694	1,231,694	224,442	204,380
113	KOSI07+FU+R4	615,916	15	1,231,862	1,231,862	224,610	204,548
114	SCHN05+F3X4+R3	616,067	22	1,232,178	1,232,178	224,926	204,864
115	GY+F1X4+I	616,171	15	1,232,372	1,232,372	225,120	205,058
116	MG+F1X4+R2	616,483	15	1,232,997	1,232,997	225,745	205,683
117	MG+F1X4+G4	616,887	14	1,233,801	1,233,801	226,549	206,487
118	MG+F1X4+I+G4	616,889	15	1,233,808	1,233,808	226,556	206,494
119	SCHN05+F1X4+R5	617,068	20	1,234,176	1,234,176	226,924	206,862
120	KOSI07+FU+R3	617,300	13	1,234,626	1,234,626	227,374	207,312
121	MGK+F1X4	617,351	14	1,234,730	1,234,730	227,478	207,416
122	GY+F1X4	617,744	14	1,235,515	1,235,515	228,263	208,201
123	KOSI07+F3X4+I	618,072	19	1,236,181	1,236,182	228,929	208,868
124	SCHN05+F1X4+R4	618,974	18	1,237,984	1,237,984	230,732	210,670
125	MG+F3X4+I	619,182	20	1,238,403	1,238,403	231,151	211,089
126	KOSI07+F3X4	619,604	18	1,239,244	1,239,244	231,992	211,930
127	KOSI07+F1X4+R2	619,779	14	1,239,585	1,239,585	232,333	212,271
128	SCHN05+F+I	619,826	70	1,239,792	1,239,792	232,540	212,478
129	MG+F3X4	620,567	19	1,241,172	1,241,172	233,920	213,858

Continued on next page

Table S1 – *Continued from previous page*

Rank	Model	$-\ln(\mathcal{L})$	df	AIC	AICc	ΔAIC	ΔAICc
130	SCHN05+F	620,670	69	1,241,477	1,241,477	234,225	214,163
131	KOSI07+F1X4+G4	620,863	13	1,241,751	1,241,751	234,499	214,437
132	KOSI07+F1X4+I+G4	620,862	14	1,241,753	1,241,753	234,501	214,439
133	SCHN05+F1X4+R3	621,059	16	1,242,150	1,242,150	234,898	214,836
134	MG+F1X4+I	622,158	14	1,244,344	1,244,344	237,092	217,030
135	KOSI07+FU+R2	622,429	11	1,244,879	1,244,879	237,627	217,565
136	SCHN05+F3X4+R2	623,050	20	1,246,140	1,246,140	238,888	218,826
137	SCHN05+FU+R10	623,378	27	1,246,810	1,246,810	239,558	219,496
138	SCHN05+F1X4+R2	623,541	14	1,247,111	1,247,111	239,859	219,797
139	MG+F1X4	623,675	13	1,247,376	1,247,376	240,124	220,062
140	SCHN05+FU+R9	623,893	25	1,247,836	1,247,836	240,584	220,522
141	KOSI07+FU+G4	624,314	10	1,248,647	1,248,647	241,395	221,333
142	KOSI07+FU+I+G4	624,313	11	1,248,647	1,248,647	241,395	221,333
143	SCHN05+F1X4+G4	624,399	13	1,248,823	1,248,823	241,571	221,509
144	SCHN05+F1X4+I+G4	624,398	14	1,248,825	1,248,825	241,573	221,511
145	SCHN05+FU+R8	624,408	23	1,248,861	1,248,861	241,609	221,547
146	SCHN05+FU+R7	624,916	21	1,249,874	1,249,874	242,622	222,560
147	KOSI07+F1X4+I	625,424	13	1,250,875	1,250,875	243,623	223,561
148	SCHN05+FU+R6	625,486	19	1,251,009	1,251,009	243,757	223,695
149	SCHN05+FU+R5	626,269	17	1,252,572	1,252,572	245,320	225,258
150	SCHN05+F3X4+G4	626,387	19	1,252,812	1,252,812	245,560	225,498
151	SCHN05+F3X4+I+G4	626,387	20	1,252,813	1,252,813	245,561	225,499
152	KOSI07+F1X4	627,290	12	1,254,605	1,254,605	247,353	227,291
153	SCHN05+FU+R4	627,433	15	1,254,896	1,254,896	247,644	227,582
154	KOSI07+FU+I	627,802	10	1,255,624	1,255,624	248,372	228,310
155	SCHN05+FU+R3	628,994	13	1,258,014	1,258,014	250,762	230,700
156	KOSI07+FU	630,149	9	1,260,316	1,260,316	253,064	233,002
157	SCHN05+FU+R2	632,325	11	1,264,673	1,264,673	257,421	237,359

Table S1 – *Continued from previous page*

Rank	Model	$-\ln(\mathcal{L})$	df	AIC	AICc	ΔAIC	ΔAICc
158	SCHN05+F3X4+I	632,477	19	1,264,991	1,264,991	257,739	237,677
159	SCHN05+F1X4+I	633,183	13	1,266,392	1,266,392	259,140	239,078
160	SCHN05+FU+G4	633,625	10	1,267,270	1,267,270	260,018	239,956
161	SCHN05+FU+I+G4	633,625	11	1,267,272	1,267,272	260,020	239,958
162	SCHN05+F3X4	633,952	18	1,267,940	1,267,940	260,688	240,626
163	SCHN05+F1X4	635,039	12	1,270,102	1,270,102	262,850	242,788
164	SCHN05+FU+I	640,485	10	1,280,991	1,280,991	273,739	253,677
165	SCHN05+FU	643,334	9	1,286,686	1,286,686	279,434	259,372
166	GTR+G	655,116	610	1,311,553	1,311,554	304,301	284,240

Simulations

As stated in the main text, overall, the simulation results indicate that the SelAC model can reasonably recover the known values of the generating model (Figure S3 - S5). This includes not only the parameters in SelAC, but also the optimal amino acids for a given sequence as well as the estimates of the branch lengths. Aside from the observations noted in the main text, a reviewer pointed out to us that it may also be difficult for SelAC to account for changing amino-acid, which we agree may also play a role. It has been suggested, in studies of the behavior of the gamma distribution in applications of nucleotide substitution model, that increasing the number of rate categories can often improve accuracy of the shape parameter (Mayrose *et al.* (2005)). Future work will address this issue.
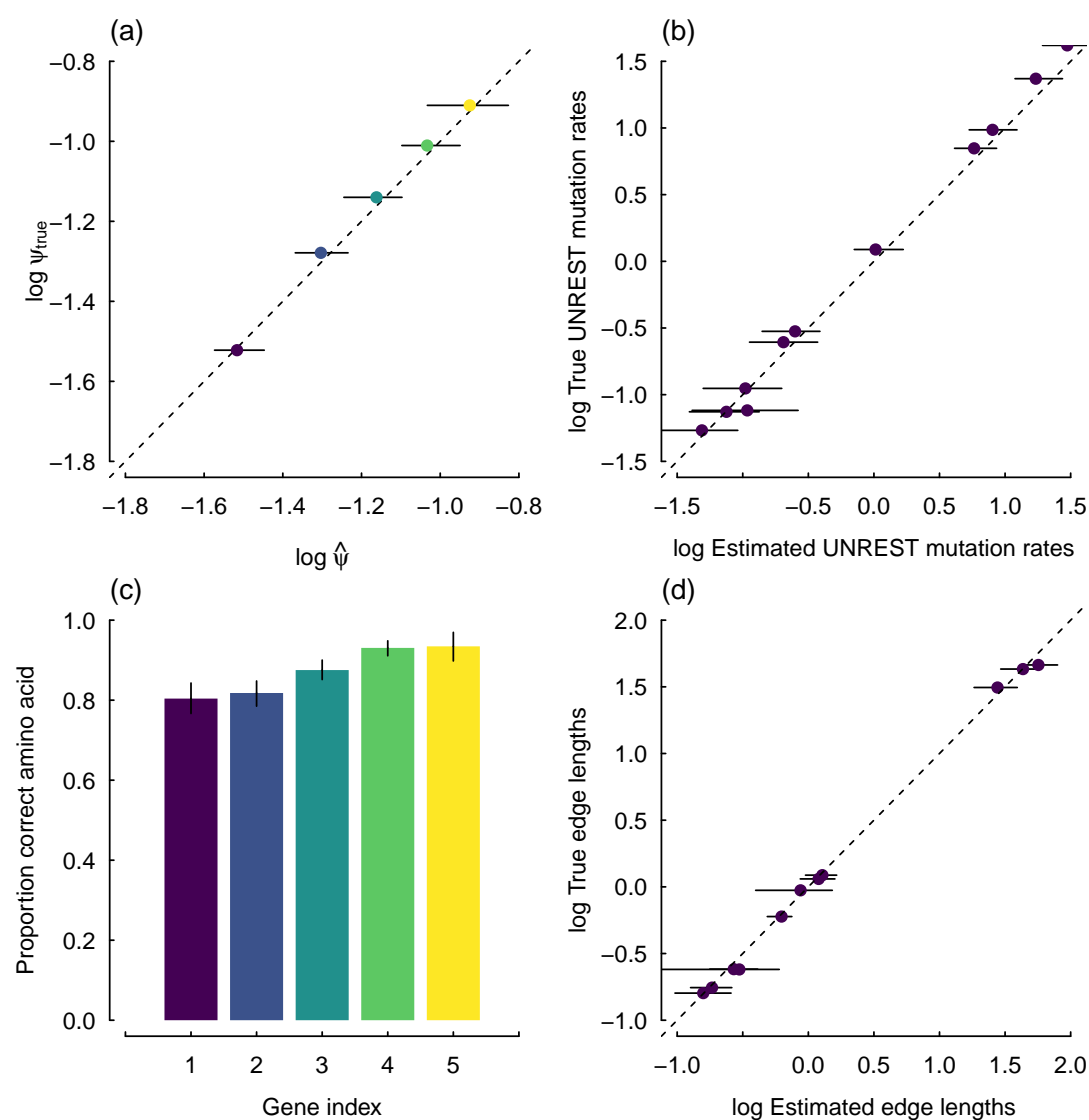

FIG. S3. Same figure as in Figure 1 in the main text, except the generating model does not include a site-specific sensitivity in the generating model (i.e., $\alpha_G = \infty$).
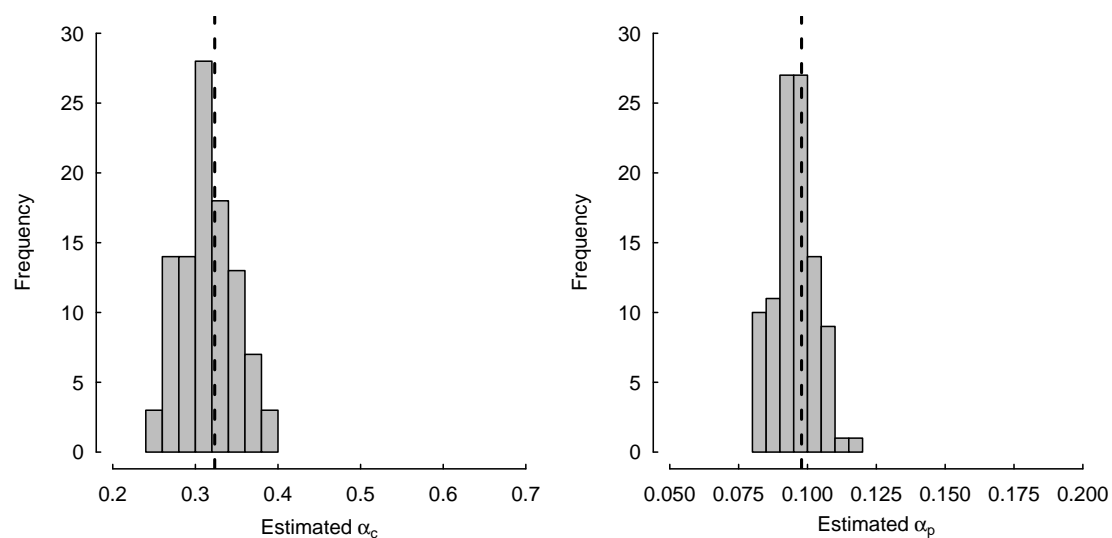
FIG. S4. The distribution of estimates of the Grantham weights, α_c and α_p, in a SelAC model, where we assume $\alpha_G = \infty$, and thus no site-specific sensitivity in the generating model. The dashed line represents the value used in the generating model.
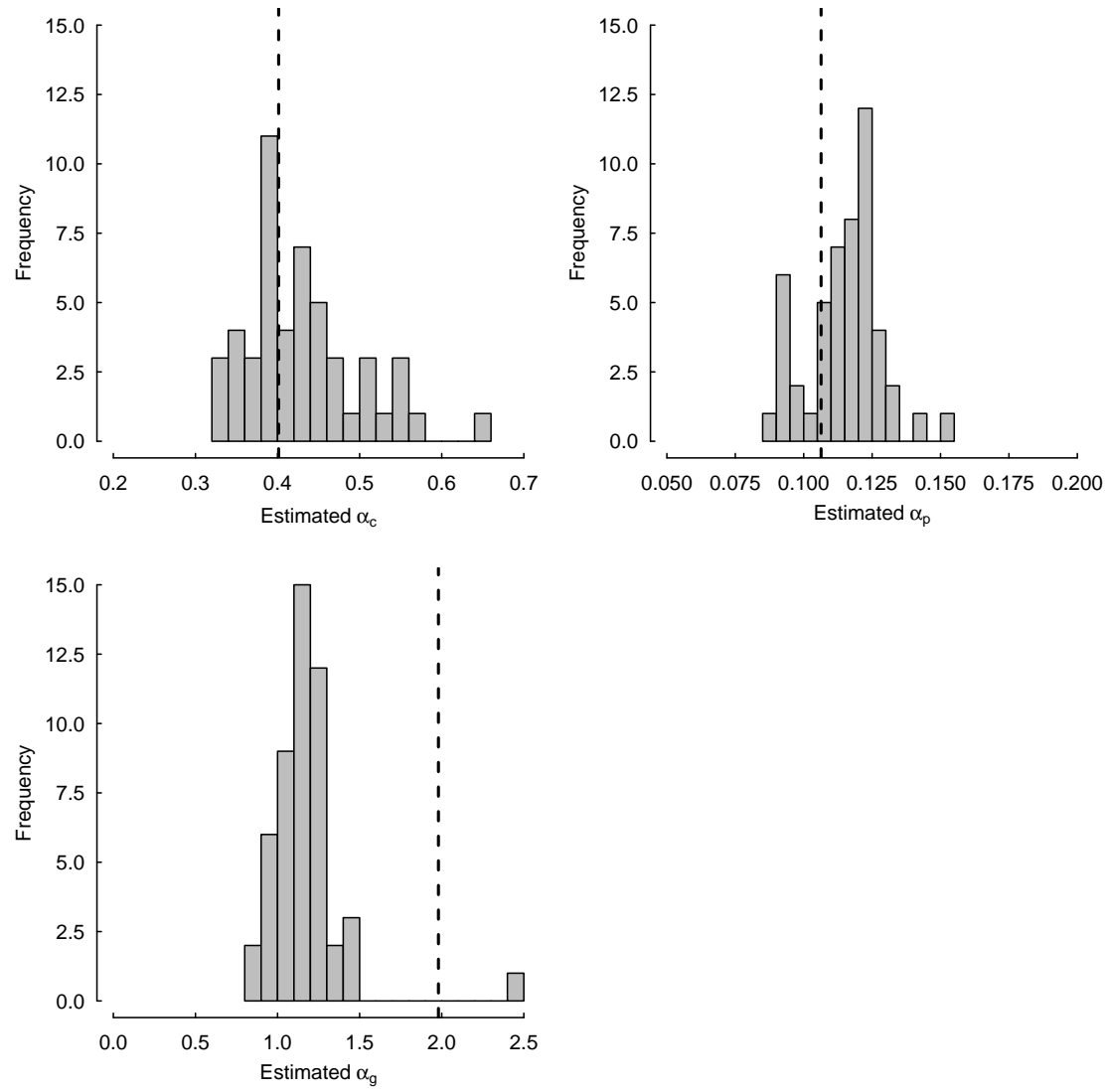
FIG. S5. Same figure as in Figure S4, except the generating model includes site-specific sensitivity in the generating model (i.e., α_G). Unlike, Grantham weights, which showed no systematic bias, there is a downward bias in estimates of α_G.